Abdominal Radiology (2019) 44:1644–1674
https://doi.org/10.1007/s00261-019-01930-7

REVIEW

Ischiorectal fossa: benign and malignant neoplasms of this "ignored" radiological anatomical space

S. C. Faria[1,3] · S. B. Elsherif[1] · T. Sagebiel[1] · V. Cox[1] · B. Rao[1] · C. Lall[2] · P. R. Bhosale[1]

Published online: 6 April 2019

Abstract

Purpose To review the pertinent anatomy and the imaging features of common and uncommon benign and malignant neoplasms and masses of the ischiorectal fossa.

Results The ischiorectal or ischioanal fossa is the largest space in the anorectal region. The benign neoplasms that develop in the ischiorectal originate from the different components that forms the fossa including vascular tumors such as aggressive angiomyxoma or hemangioma; neural tumors as plexiform neurofibroma or schwannoma; fat tumors as lipoma; skin/skin appendages tumors as hidradenoma papilliferum; smooth or skeletal muscle tumors as solitary fibrous tumor. The malignant neoplasms that develop in the ischiorectal fossa also originate from different components that forms the fossa including vascular tumors such as angiosarcoma, neural tumors as malignant granular cell tumor and malignant peripheral nerve sheath tumor; fat tumors as liposarcoma; smooth or skeletal muscle tumors as leiomyosarcoma, rhabdomyosarcoma, malignant PEComa, or undifferentiated pleomorphic sarcoma. Additionally, the ischiorectal fossa can also harbor secondary hematogenous metastases and be affected by direct invasion from neoplasms of adjacent pelvic organs and structures. Furthermore, other miscellaneous masses can occur in the ischiorectal fossa including congenital and developmental lesions, and inflammatory and infectious processes.

Conclusion Knowledge of the anatomy, and the spectrum of imaging findings of common and uncommon benign and malignant neoplasms of the ischiorectal fossa is crucial for the radiologists during interpretation of images allowing them to make contributions to the diagnosis and better patient management.

Keywords Ischiorectal fossa · Anorectal space · Aggressive angiomyxoma · Plexiform neurofibroma · Liposarcomas · Malignant granular cell tumors

Introduction

The ischiorectal or ischioanal fossa is the largest space in the anorectal region. It is a pyramidal shaped space situated bilaterally to the inferior aspect of the rectum and anus with its base directed to the surface of the perineum and its apex directed anteromedially towards the pubic symphysis [1].

Neoplastic lesions of the ischiorectal fossa are rare, however, a wide range of benign and malignant tumors and masses (Figs. 1, 2) can occur in the ischiorectal fossa making it important to discuss this space. The neoplasms that develop in the ischiorectal originate from the different components that form the fossa including vessels, nerves, fat, skin, and muscles. The benign neoplasms (Fig. 1) include vascular tumors as aggressive angiomyxoma or hemangioma; neural tumors as plexiform neurofibroma or schwannoma; fat tumors as lipoma; skin/skin appendages tumors as hidradenoma papilliferum; and smooth or skeletal muscle tumors as solitary fibrous tumor. The malignant neoplasms (Fig. 2) that develop in the ischiorectal fossa also originate from the different components of the fossa including vessels, nerves, fat, skin, and muscles. They include vascular

CME activity This article has been selected as the CME activity for the current month. Please visit https://ce.mayo.edu/node/82514 and follow the instructions to complete this CME activity.

✉ S. C. Faria
scfaria@mdanderson.org

[1] Department of Diagnostic Radiology, The University of Texas M. D. Anderson Cancer Center, Houston, TX, USA

[2] University of Florida, Jacksonville, FL, USA

[3] 1400 Pressler St. Unit 1473, Houston, TX 77030, USA

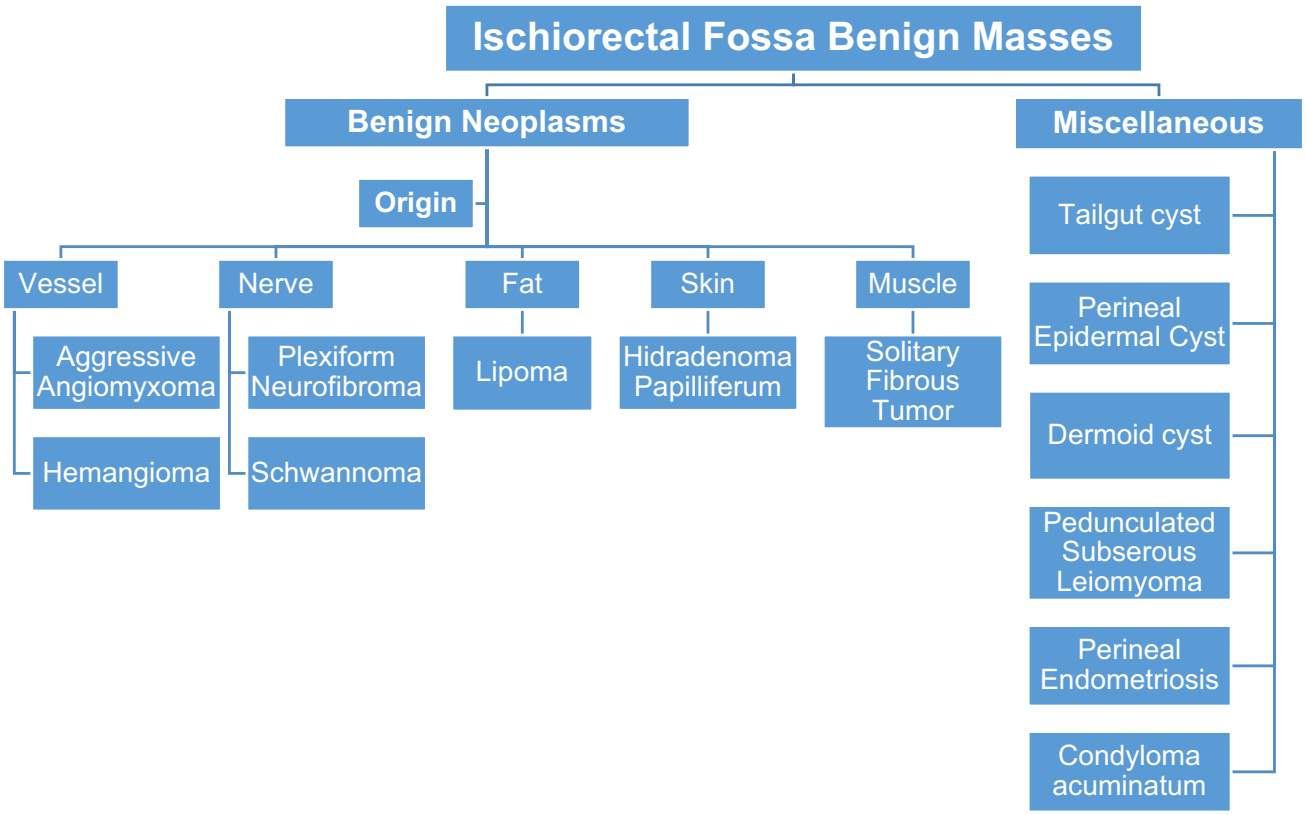

Fig. 1 Differential diagnosis of ischiorectal fossa benign neoplasms and miscellaneous masses

tumors as angiosarcoma, neural tumors as malignant granular cell tumor and malignant peripheral nerve sheath tumor; fat tumors as liposarcoma; and smooth or skeletal muscle tumors as leiomyosarcoma, rhabdomyosarcoma, malignant PEComa, or undifferentiated pleomorphic sarcoma. Additionally, the ischiorectal fossa can also harbor secondary hematogenous metastases and be affected by direct invasion from neoplasms of adjacent pelvic organs and structures. Furthermore, other miscellaneous masses can occur in the ischiorectal fossa including congenital and developmental lesions, and inflammatory and infectious processes [2].

Cross-sectional imaging plays a crucial role in depicting the anatomy and evaluating the extent of disease involving the ischiorectal fossa. Computed tomography (CT) and magnetic resonance imaging (MRI) are essential in the evaluation of pathologies affecting the ischiorectal fossa defining the size, anatomic origin, and relationship to adjacent structures, extent, and internal characteristics of the benign and malignant neoplasms of the ischiorectal fossa. Most recently, Fluro-deoxy-glucose Positron Emission Tomography (FGD-PET) helps in the functional evaluation of the neoplastic masses [3].

Knowledge of the anatomy of the ischiorectal fossa allows a better understanding of the benign and malignant neoplasms and masses that may arise from it. In this pictorial essay, we review the pertinent anatomy and anatomic landmarks of the ischiorectal fossa, discus the roles of different images modalities and illustrate the characteristic imaging features of common and uncommon benign and malignant neoplasms and masses that originate primarily within the ischiorectal fossa and the secondary involvement by other pathologies from adjacent pelvic organs affecting the ischiorectal fossa. This knowledge will contribute to the differential diagnosis and interpretation of the images allowing a better care and management of the patients.

Normal anatomy

The ischiorectal fossa is the largest space in the anorectal region. The right and left ischiorectal spaces communicate posteriorly through the deep postanal (retro-sphincteric) space [1]. It is bounded medially and superiorly by the levator ani muscle and medially by the external anal sphincter muscles; laterally by obturator internus muscle and obturator fascia; anteriorly by the superficial and deep transverse perineal muscles; posteriorly by the lower border of gluteus maximus muscle and the sacrotuberous ligament; and inferiorly by the skin of the perineum [1–3]. The ischiorectal

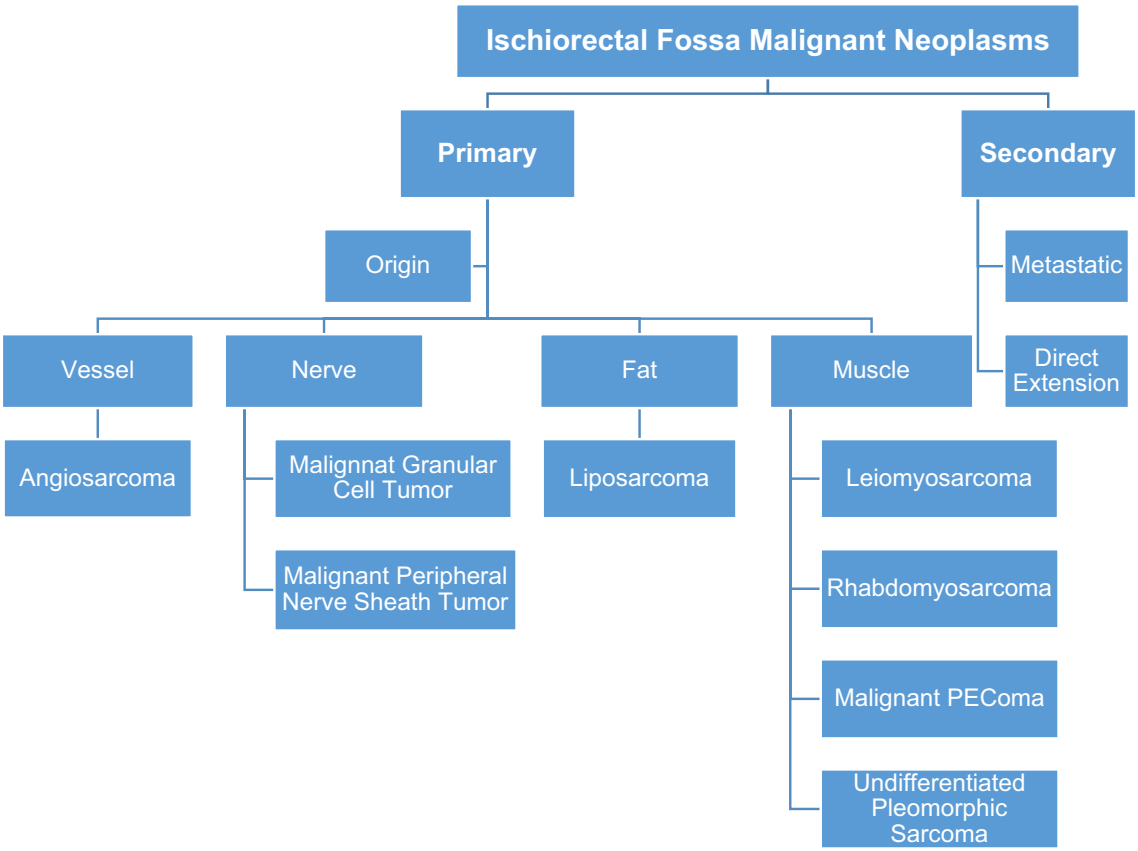

Fig. 2 Differential diagnosis of ischiorectal fossa malignant neoplasms

fossa is supplied by the rectal and scrotal or labial branches of the internal pudendal vessels, in addition to the branches of the pudendal nerve [3, 4]. The pudendal canal runs along the lower lateral wall of the ischiorectal fossa, just medial to the obturator internus muscle and transmits the pudendal nerves and internal pudendal artery and vein.

The contents of the ischiorectal fossa include adipose tissue, vessels, lymphatics trunks, and nerves. The lobulated adipose tissue acts as fat bearing for the rectal and anal motions. Moreover, the pumping action of this space can increase the lymphatic drainage of the region to the internal iliac lymph nodes, enhancing the spread of rectal carcinoma [4]. Understanding the anatomy of the ischiorectal fossa is crucial for compiling a differential diagnosis of a wide variety of pathologies that can occur at that location and can also be used for treatment planning. [3, 4] (Figs. 3, 4).

Benign neoplasms

Aggressive angiomyxoma

Aggressive angiomyxoma is the most common primary tumor in the ischiorectal fossa [3]. It is a benign mesenchymal tumor that has a gelatinous appearance macroscopically. Microscopically, it is formed of spindle cells, stellate cells, and scattered vessels in a myxoid background of collagen fibers, without nuclear atypia or mitosis [2, 3].

Aggressive angiomyxoma usually has specific clinical and radiological features. They have a predilection for the perineum and pelvis of middle-aged women and usually present as a perineal mass associated with pelvic or perineal pain, urinary frequency, or dyspareunia [5]. They are locally infiltrative tumors with finger-like projections displacing nearby structures, but they don't have a metastatic potential [3, 5, 6].

On ultrasound, angiomyxoma appears as hypoechoic soft tissue mass that may present some cystic features [5]. On CT, it presents as a well-defined iso- or hypoattenuating mass with swirling internal pattern on post-contrast images, or cystic appearing mass with some solid components [2, 7]. MRI features include iso- to hypointense signal intensity relative to the muscle on T1WIs; high signal intensity on T2WIs (due to the myxoid matrix) with the characteristic "swirling" or "laminated" pattern consisting of alternating layers of lower intensity component within the high signal tumor; in addition to a heterogeneous avid post-contrast enhancement (Fig. 5) [3, 7–9]. On imaging, the tumor usually displaces neighboring pelvic structures without direct

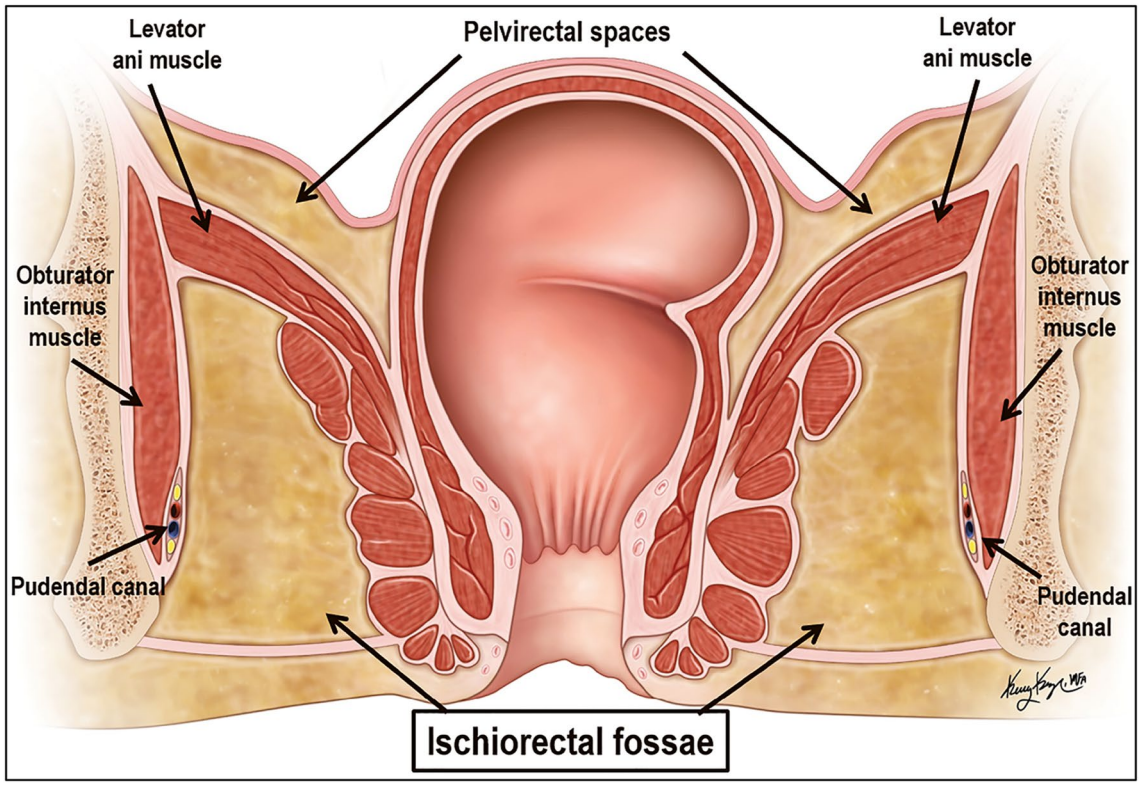

Fig. 3 Illustration of the anatomy of the ischiorectal fossa

invasion [2, 3] [7]. They are treated with surgical resection but approximately 70% of angiomyxoma cases recur after 2 years [7]. Although these tumors are not malignant, Satheshkumar et al. [6] described a rare case of angiomyofibrosarcoma in the ischiorectal fossa, in which histological examination revealed low-grade sarcomatous changes in an undetermined pre-existing lesion of angiomyxoma or angiomyofibroblastoma [6].

Vascular anomalies

Vascular anomalies are divided into vascular malformations and hemangiomas based on their endothelial origin [10, 11]. Vascular malformations are developmental anomalies that often result from abnormal development in the blood vessels and they persist or grow slowly. Meanwhile, hemangiomas are true neoplasms that expand rapidly postnatal and regress slowly during childhood [10]. Hemangiomas and vascular malformations rarely develop in the ischiorectal fossa [12].

MRI is the modality of choice to depict vascular anomalies in the ischiorectal fossa as it can also help to diagnose hemangiomas and to differentiate between slow-flow and high-flow vascular malformations (Fig. 6) [11]. Hemangiomas appear as bright lesion on T2WI. Slow-flow venous malformations appear bright on fat-suppressed T2WIs, while high-flow arterial malformations contain signal voids that represent phlebolith and calcifications [10]. In addition, post-contrast T1 sequence in MRI shows enhancing vessels with signal voids [10]. Vascular malformations may be associated with syndromes such as Klippel–Trénaunay syndromes [11].

Plexiform neurofibroma

Plexiform neurofibroma is an overgrowth of endoneurial myxomatous tissue, Schwann cells and collagen fibers that form multiple masses along the course of the affected nerves [13]. They are pathognomonic of neurofibromatosis type 1 (NF1) [14]. Plexiform neurofibroma commonly involves extremities, neck, mediastinum, and pelvis [2].

Pelvic plexiform neurofibroma involving the pudendal nerve presents as a mass in the ischiorectal fossa which can also displace the bladder and rectum [2]. They appear as poorly enhancing masses with low attenuation on CT images [2, 13]. MRI is the modality of choice to show the size and actual extent of plexiform neurofibromas [14].

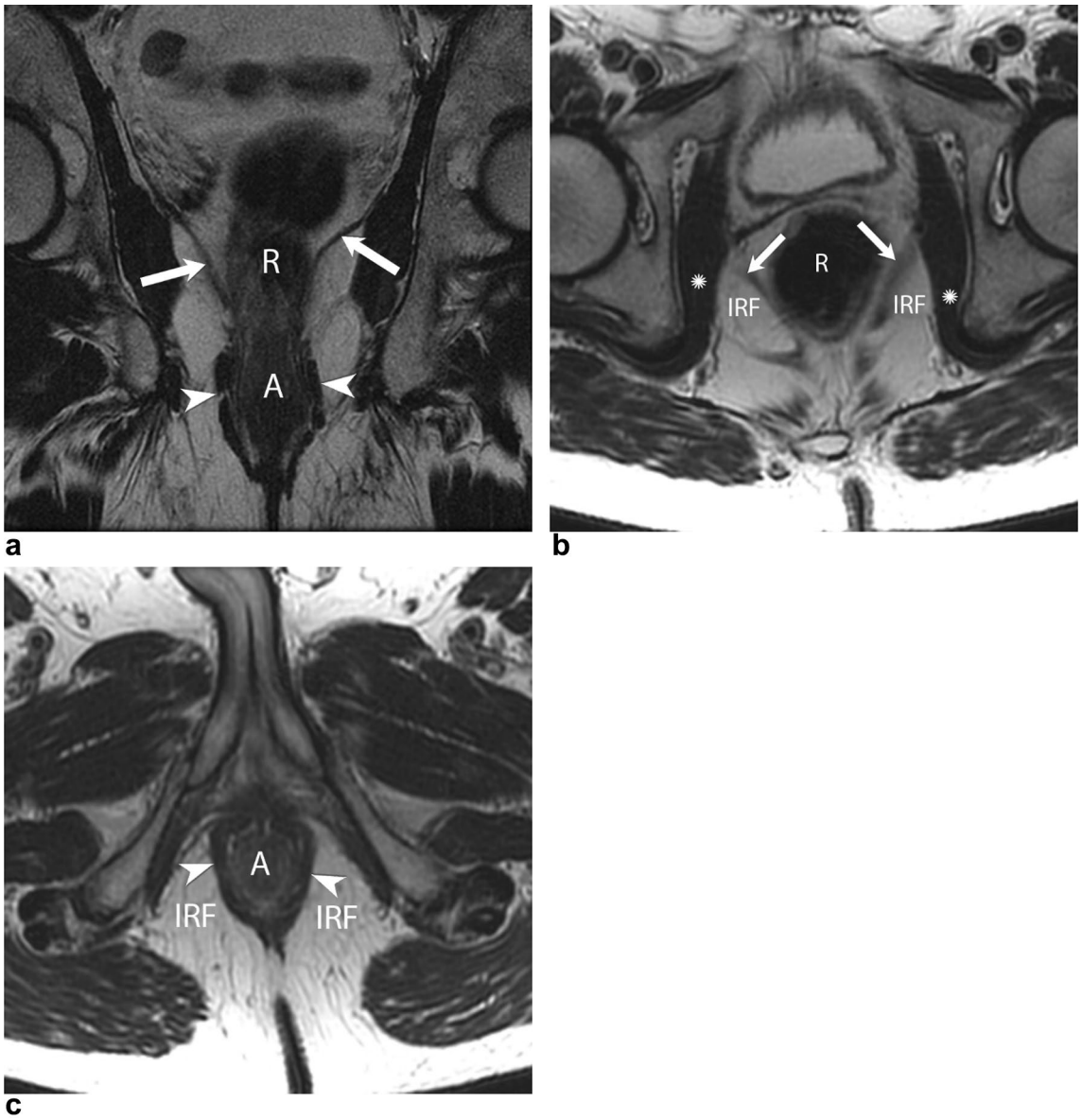

Fig. 4 Ischiorectal fossa anatomy. MRI pelvic images depicting the anatomical location and boundaries of the ischiorectal fossa. **a** Coronal T2WI shows the levator ani muscle (white arrows) that forms the superior border of the ischiorectal fossa and the external anal sphincter (white arrowheads) that limits its medial borders. **b** Axial T2WI shows the levator ani muscle (white arrow) and the obturator internus muscles (*) that outline the IRF laterally. **c** Axial T2WI shows the external anal sphincter (white arrowhead). *R* rectum, *A* anus, *IRF* ischiorectal fossa

MRI characteristics (Fig. 7) include signal intensity higher than muscle in T1WI and hyperintense signal on T2WI [13]. Moreover, neurofibromas typically have a target-like appearance on T2WI, with a central low signal intensity and peripheral high signal intensity [15]. T1WI shows hyperintense intratumoral septations which correspond to the myelinated axons [13]. Furthermore, MRI can distinguish the thickened perineurium surrounding the tumor [13]. A plexiform neurofibroma can undergo sarcomatous transformation into malignant peripheral nerve sheath tumors (MPNSTs) [13].

Schwannoma

Schwannomas are benign encapsulated nerve sheath neoplasms that arise from cranial nerves as well as peripheral nerves of the neck, mediastinum, and extremities [16].

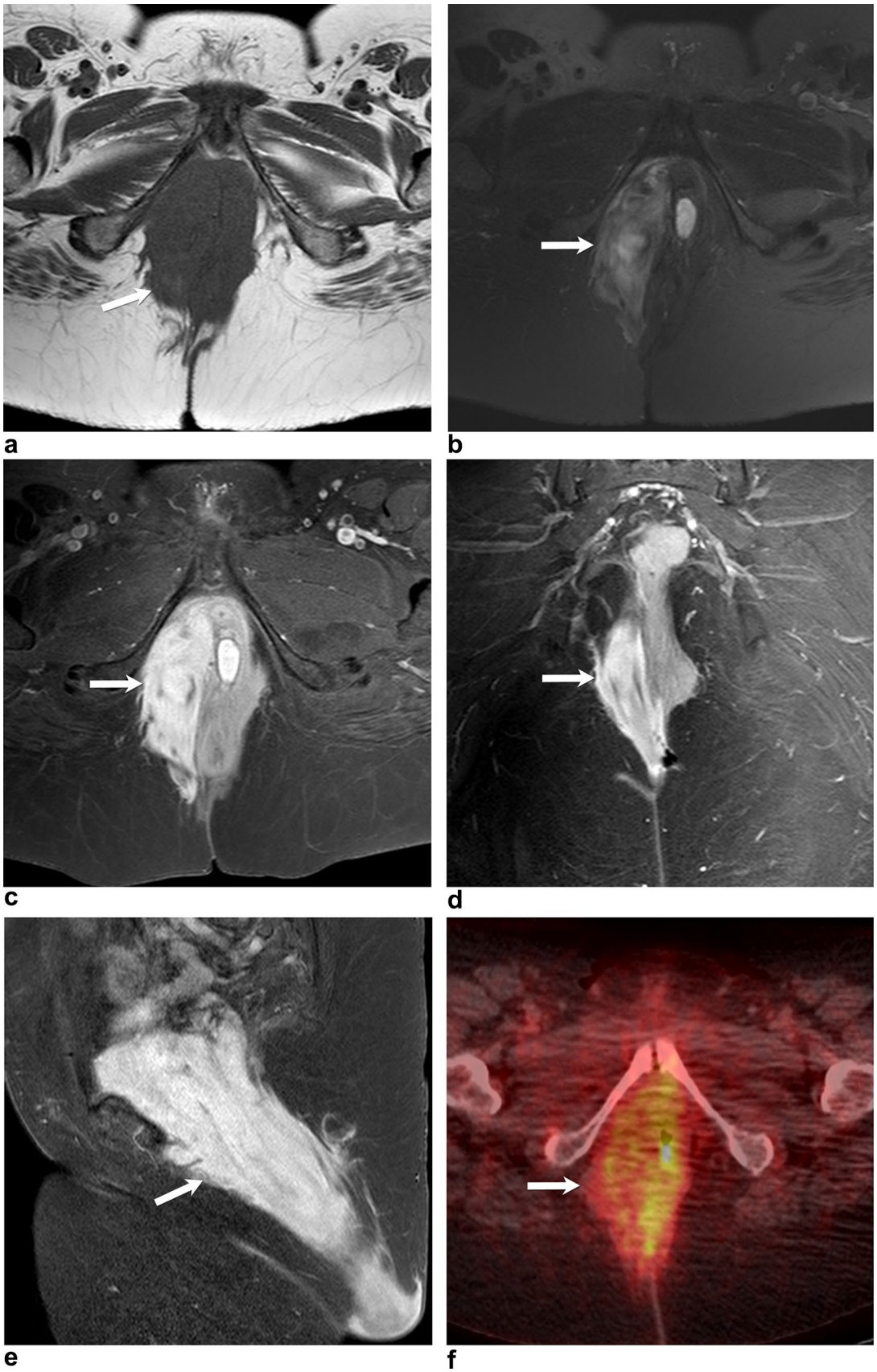
a
b
c
d
e
f

◂**Fig. 5** 60-year-old female with a pelvic mass. **a**–**c** Pelvic MRI, Axial T1WI (**a**) and axial SPIR T2WI (**b**) showing a large mass (white arrow) in the right ischiorectal fossa with low signal in T1WI and high signal in T2WI (white arrow) with intense enhancement in post-contrast T1WI (white arrow) (**c**). **d**, **e** Pelvic MRI, Coronal (**d**) and Sagittal (**e**) post-contrast T1WIs demonstrate the mass (white arrow) extending from the ischiorectal fossa to the right gluteal region. Note the laminated appearance. **f** Axial PET/CT image shows the aforementioned mass (white arrow) with low level FDG uptake. Biopsy confirmed the diagnosis of aggressive angiomyxoma

Pelvic schwannoma arising from the pudendal nerve is a rare entity of peripheral schwannomas [16]. Histopathologically, schwannoma is composed of spindle cells characterized by elongated or ovoid nuclei and no atypia [17, 18]. Schwannomas are usually discovered incidentally as a large perineal mass. However, they can present occasionally with non-specific pelvic pain, mass, or pressure symptoms as dysuria or dyschezia [17].

Schwannoma appears as a well-circumscribed ovoid or spherical mass on CT images with heterogeneous contrast enhancement [17, 18]. MRI features of schwannoma include low signal on T1WIs; high signal on T2WIs; and heterogeneous contrast enhancement (Fig. 8) [17, 19]. Schwannomas are non-aggressive lesions but incompletely resected tumors can recur [18].

Lipoma

Lipomas are the most common benign neoplasms of the soft tissues. They originate from adipose tissue [20]. Lipomas can occur almost anywhere in the body; however, it is uncommon for lipomas to arise in the ischiorectal fossa [2]. Lipomas usually present as a painless soft tissue mass [21]. On CT, lipoma has density similar to subcutaneous fat [22]. On MRI, lipoma has high signal intensity on T1WIs, low signal intensity on T2WIs, and suppressed signal on both fat-saturation and STIR sequences [20]. Some lipomas have also intratumoral fibrovascular septa that appear as soft tissue attenuation on CT and hypointense on T1WIs [2]. On imaging, large septated lobulated lipomas can be difficult to distinguish from low-grade liposarcoma [2]. Large lipomas are usually managed through surgical excision [2].

Hidradenoma papilliferum

Hidradenoma papilliferum is a rare benign tumor of cutaneous appendages which usually involve the anogenital region. It arises from mammary-like apocrine glands around the anus and vulva [21, 23]. Hidradenoma papilliferum is usually asymptomatic, but may present with itching, or discharge and bleeding in case of ulcerating large lesions [24]. Radiological features (Fig. 9) include a hypodense lesion on CT and a hypointense lesion on T1WI and hyperintense lesion on T2WI on MRI [23]. Although the malignant change of hidradenoma papilliferum to adenocarcinoma or adenosquamous carcinoma has rarely been reported, surgical resection remains the definitive therapy [23, 24].

Solitary fibrous tumor

Solitary fibrous tumors (previously called hemangiopericytomas) are rare tumors of mesenchymal origin that usually has a hemangiopericytoma-like vascular pattern [25, 26]. Although they usually arise in the pleura, extrapleural tumors have occasionally been reported [27]. Myxoid solitary fibrous tumor is a rare histological subtype of these uncommon neoplasms [25]. In 2003, Yap et al. [25] presented a case of myxoid solitary fibrous tumor in the ischiorectal fossa in a 41-year-old man who presented with a progressively enlarging perianal lump [25]. Although extrapleural solitary fibrous tumors are often benign, [25] 20% of these tumors can be malignant [28]. Malignant features include marked cellular atypia and mitosis, in addition to infiltrative growth pattern [29].

On MRI, solitary fibrous tumors often show iso- or hypointense signal on T1WI; heterogenous signal intensity on T2WIs, depending on the main element of the tumor; and heterogeneous contrast enhancement (Fig. 10) [29, 30]. The low T2 signal intensity correlates with the high collagen content of the tumor. Meanwhile, the high T2 signal intensity is linked to myxoid degeneration and hypercellularity of the tumor [30]. CT shows circumscribed lobulated isodense soft-tissue mass with some occasional dispersed calcifications and variable enhancement on contrast-enhanced images. Moreover, the tumor might demonstrate some hypodense areas which correlate with cystic or necrotic changes [28]. Furthermore, FDG-PET is a helpful tool in the staging of these tumors, in addition to differentiating benign, low- and high-grade lesions. Benign solitary fibrous tumors are managed by complete surgical resection and they may recur in 10–15% of cases [25].

Miscellaneous benign lesions

Tailgut cyst

Tailgut cyst, also known as retrorectal cystic hamartoma, is a rare congenital anomaly that arises from remnants of the embryonic hindgut (tailgut) [3]. It is usually located in the retrorectal space above the levator ani but it can occasionally descend along the posterolateral border into the ischiorectal fossa [3, 12]. Grossly, tailgut cyst is a unilocular or

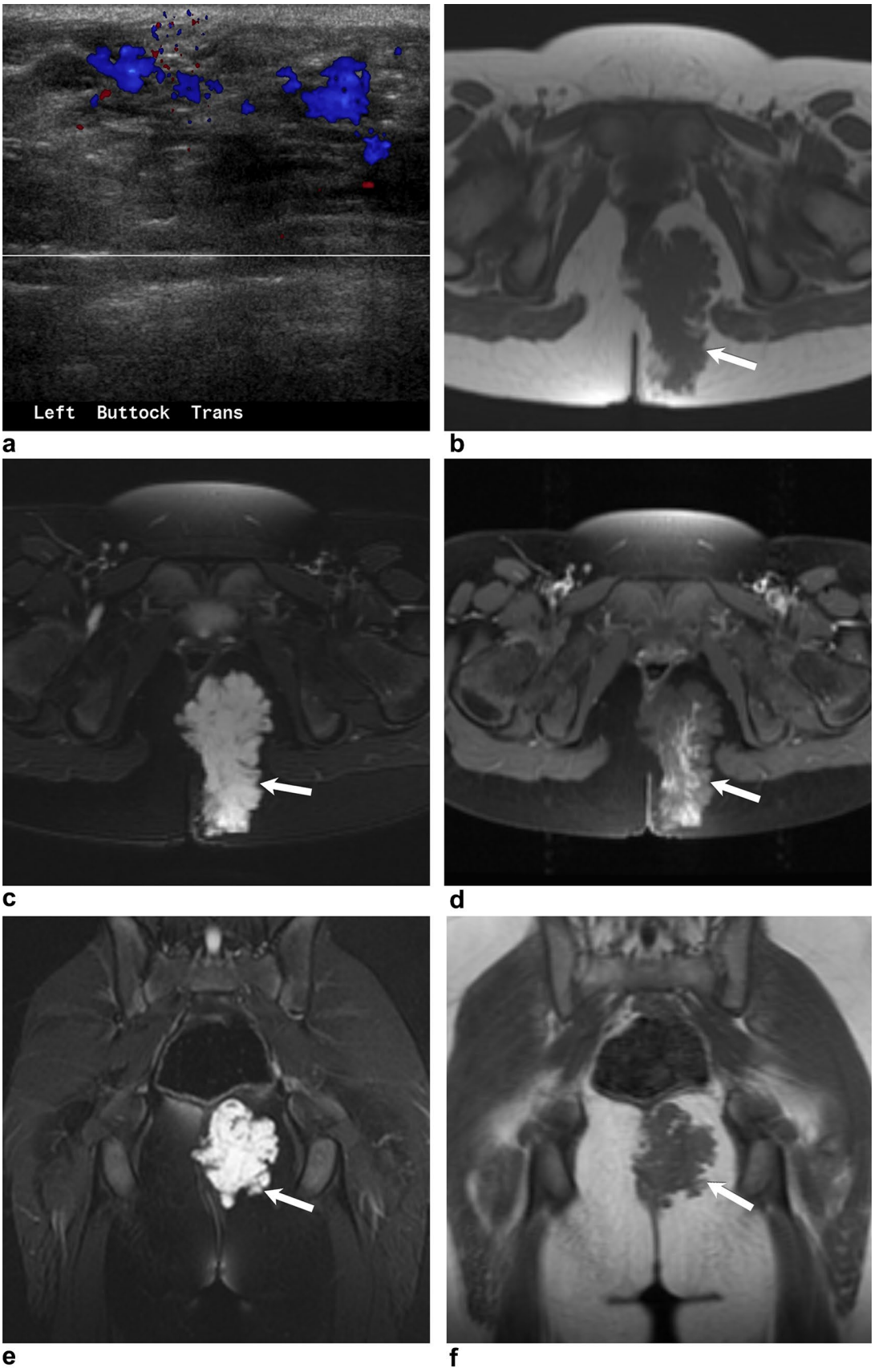
Left Buttock Trans
a
b
c
d
e
f

◂**Fig. 6** 6-year-old female presents with a discoloration on the left buttock. **a** Ultrasonography image showing serpiginous vessels (arrow) within the subcutaneous tissues of the left buttock region. **b–d** Pelvic MRI, Axial T1WI (**b**), T2WI (**c**) and post-contrast T1WI (**d**) show a lobulated soft tissue mass (white arrows) with serpiginous and tubular structures, measuring approximately 6 cm × 4.9 cm in the subcutaneous fat of the left ischiorectal fossa. The mass shows T1 hypointense signal similar to the muscle, diffuse T2 hyperintense signal, and enhancement of the core of the lesion on the post-contrast image. This mass abuts and displaces the rectum to the right. **e**, **f** Pelvic MRI, Coronal T1WI (**e**) and T2WI (**f**) show the lobulated contours of the mass (white arrows) that was confirmed as hemangioma

multiseptated mass that adheres to the sacrum or the rectum without being connected with the rectal lumen. It can be lined by various epithelia that often undergo dysplastic changes [2, 3]. It is filled with clear fluid or mucoid material and it is usually surrounded by scattered bundles of smooth muscles [31].

Although tailgut cysts are usually discovered incidentally, some patients can present with rectal or perineal pain, mass on digital rectal examination, or recurrent anorectal abscesses or fistulas [2, 31]. They appear as a retrorectal complex mass with internal echoes on ultrasound imaging. On CT, tailgut cysts appear as a well-defined mass with preserved fat planes and no invasion of surrounding structures. They may have density similar to that of water or soft tissue depending on its content [2, 12, 31]. In case of infection or malignant degeneration, the tailgut cyst may show loss of discrete margins, in addition to wall thickening [31, 32]. On MRI, the tail gut cyst has a low signal intensity on T1WIs and high signal intensity on T2WIs (Fig. 11). However, T1WIs might show high signal intensity in case of hemorrhage or high protein content [32].On T2WIs, tail gut cysts have a multilocular appearance with internal septa [32].

Perineal epidermal cyst

Epidermal cysts are the most common benign cutaneous cysts. Although they can be found anywhere, they are typically seen on the scalp, face, neck, trunk, and back [33, 34]. They are pathologically classified as retention cysts of the epidermis [35]. They appear as unilocular circumscribed cysts with multilayered wall of squamous epithelium. However, unlike dermoid cysts, they don't contain specialized skin appendages such as hair follicle or sweat and sebaceous glands [34]. Although epidermal cysts are usually confined to the epidermis and subcutaneous region, they may rarely extend to the retrorectal area or ischiorectal fossa in large lesions [34, 35]. Epidermal cysts are usually slow-growing and asymptomatic except in cases of secondary infection or inflammation [33]. They are usually found incidentally in imaging studies performed for other reasons. They present as well-demarcated round or ovoid lesions with density similar of the water. Kransdorf et al. [36] reported that the presence of debris in a cystic lesion is characteristic of an epidermal cyst [36]. On MRI, they usually appear with high signal intensity on T2WI with variable low signal components and some bright foci on T1WI that usually shows central non-enhancement and peripheral thin rim enhancement after intravenous injection of contrast (Fig. 12) [3, 37].

Pedunculated subserous leiomyoma

Leiomyomas, also known as fibroids or myomas, are the most common gynecologic pathology with an incidence of 20–30% in the reproductive age women [38]. Leiomyoma is a benign neoplasm that is composed of whorled smooth muscles and fibrous stroma anchored in the uterine muscular wall [38]. These tumors are not encapsulated, but they appear well-circumscribed and enclosed by a pseudocapsule [38]. According to their location, leiomyomas are divided into submucosal, intramural, or subserosal [38]. Pedunculated subserous leiomyomas are attached to the uterus by a stalk [38]. Subserous fibroids are usually asymptomatic. However, pedunculated subserous fibroids may present with acute pain if they undergo torsion. Furthermore, they can extend between the folds of the broad ligament or even extend into the ischiorectal fossa [38].

Ultrasonography is the primary imaging modality for the diagnosis of subserous leiomyomas [39]. CT depicts well-circumscribed mass with solid consistency and attenuation values similar to the uterus (Fig. 13) [39]. Calcifications or cystic changes may appear in large tumors [39]. MRI is the most accurate imaging modality to demonstrate and localize leiomyomas [38]. They appear as a uniform hypointense mass in T2WIs and isointense on T1WIs [38, 40]. While degenerated leiomyomas have variable appearances on T1WIs, and T2WIs [38].

Perineal endometriosis

Endometriosis is the presence of ectopic endometrial tissue outside the uterine cavity [41]. Most common sites for endometriosis include peritoneal surfaces, ovaries, and uterine ligaments. It rarely involves the vulva, vagina, and perineal area [41]. Perineal endometriosis may develop at the site of previous gynecological surgery such as cesarean section, episiotomy, or laparoscopy [3].

Ultrasonography is less sensitive than MRI in the diagnosis of deep pelvic endometriosis [41]. Meanwhile, MRI has 90–92% sensitivity and 91–98% specificity for the diagnosis of endometriosis [41]. In addition, MRI is able to detect tiny masses and delineate their extent and relations

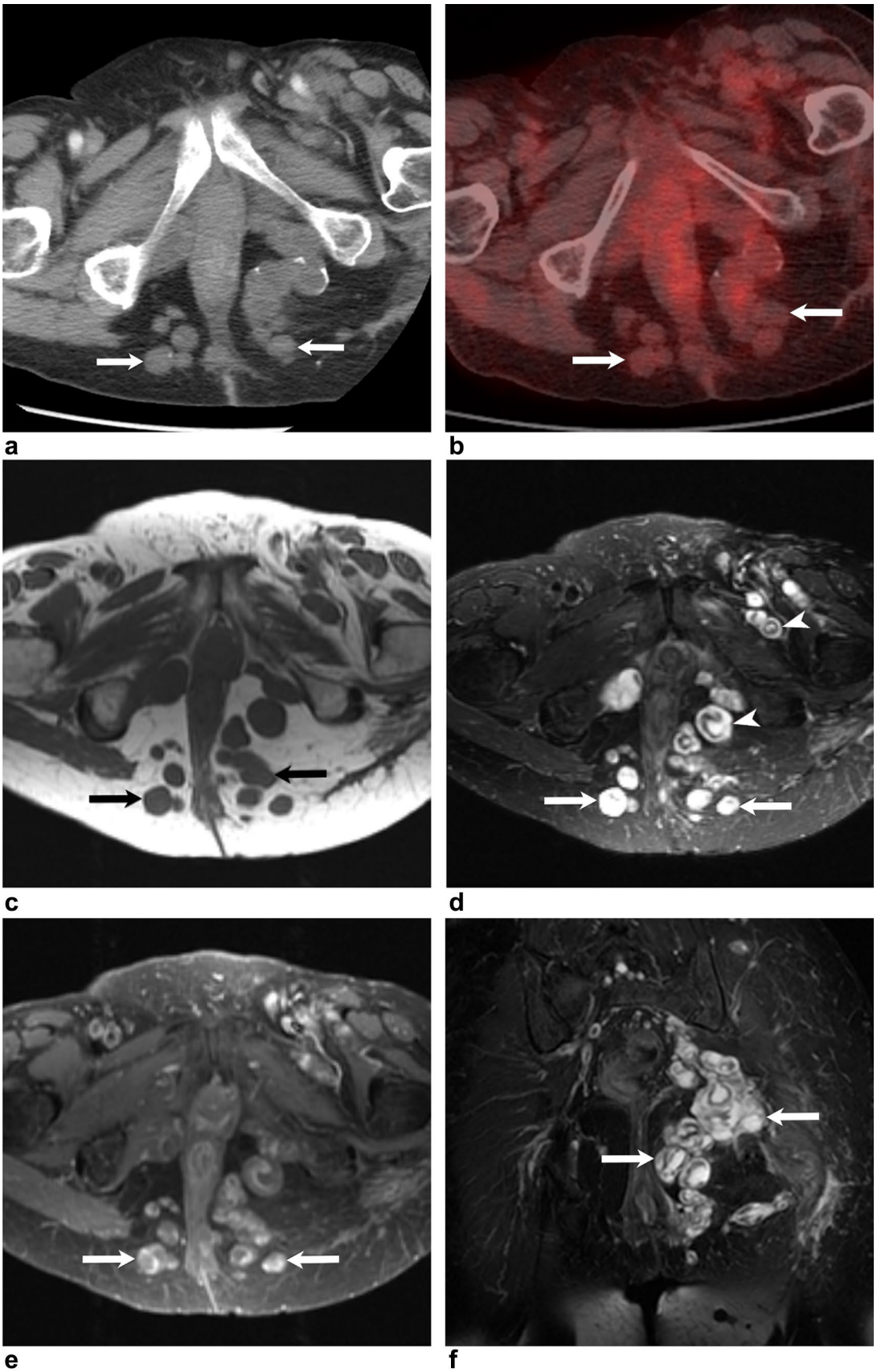
a
b
c
d
e
f

◂**Fig. 7** 65-year-old female with neurofibromatosis. **a**, **b** Axial CT image (**a**) showing multiple hypodense soft tissue nodules (arrows), some partially calcified, within the bilateral ischiorectal fossae that do not show FDG uptake on the PET/CT image (**b**). **c**–**e** Pelvic MRI, Axial T1WI (**c**), T2WI (**d**) show multiple T1-hypointense and T2-hyperintense soft tissue nodules of varying sizes (arrows) within the bilateral ischiorectal fossae. **d** Some nodules presents the target-like appearance with a central low signal and peripheral high signal intensity (arrowhead) and enhancement on the post-contrast T1WI image (**e**). **f** Pelvic MRI, Coronal T2WI shows the multiple neurofibromas

to surrounding tissues [41]. MRI features of perineal endometriosis include ill-defined nodule with hyperintense foci on T1- and T2WIs (Fig. 14) [3]. Sometimes biopsy and histological examination are necessary to exclude malignancy, particularly when endometriosis develops in post-menopausal women [41]. 0.3–1% of surgical scar endometriosis may undergo malignant transformation [42].

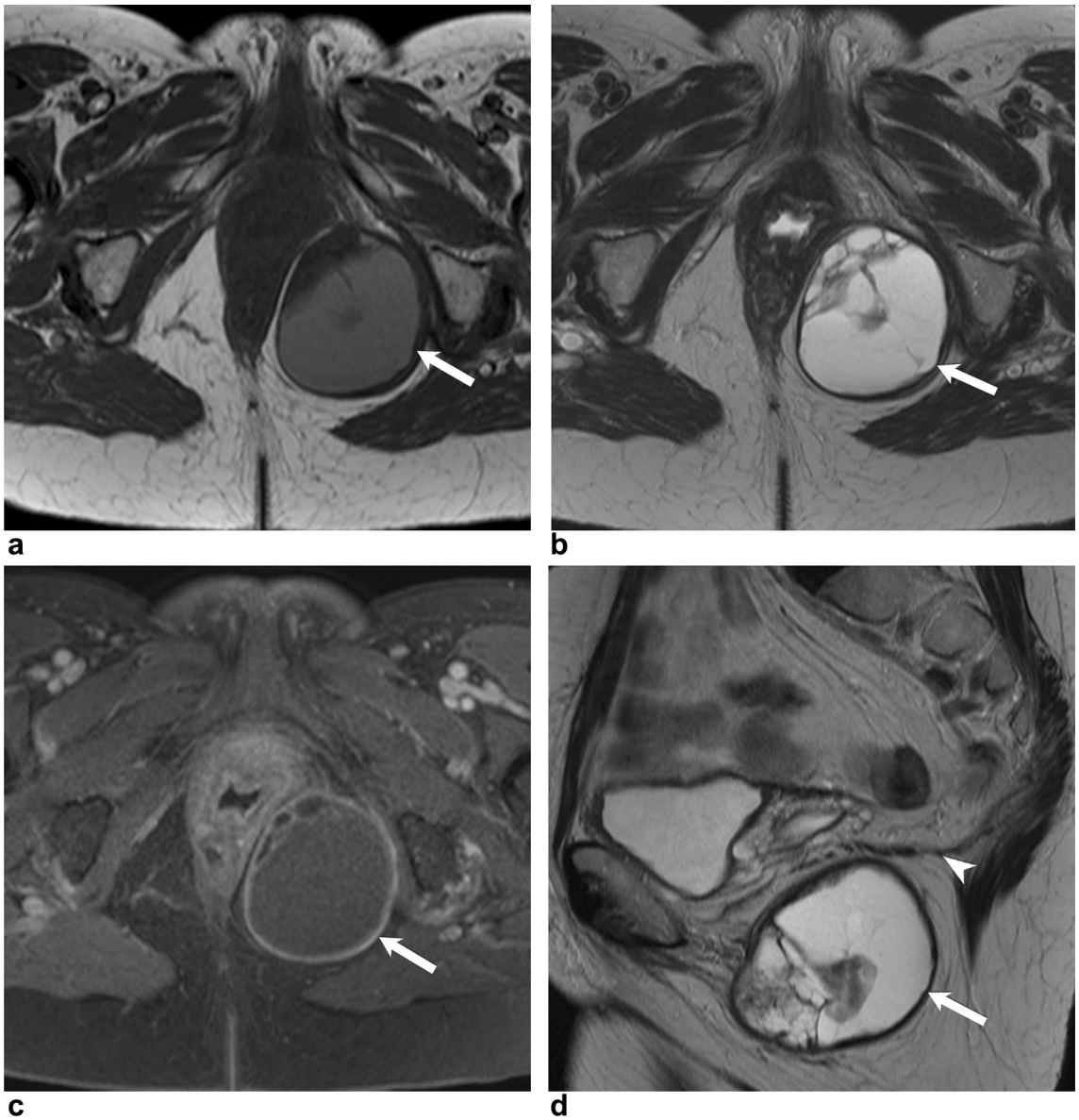

Fig. 8 65-year-old female with a pelvic mass for which she underwent MRI assessment of the pelvis. **a**, **b** Axial T1WI (**a**) and T2WI (**b**) showing a large well-circumscribed mass (white arrows) measuring 6.6 × 5.4 cm in the left ischiorectal fossa fat with intermediate signal in T1WI and increased signal in T2WI likely representing mucin, proteinaceous or myxoid content. **c** Axial post-contrast T1WI demonstrates peripheral enhancement of the mass (white arrow).**d** Sagittal T2WI shows that the mass (white arrow) abuts and is located inferior to the levator ani muscle (white arrowhead). Note the hypointense rim, likely related to fibrous tissue. Surgical resection confirmed a schwannoma

Condyloma acuminatum

External condyloma acuminata (genital warts) develop in the perianal and perigenital areas [43]. Human papilloma virus (HPV) is the causative agent of genital warts with type 6, 11, 16, and 18 are the most common associated virus strains. HPV 6 and 11 are associated with typical condyloma acuminata, while HPV 16, 18 are linked to dysplasia and malignant change [44]. They can present singularly, in clusters or in plaques. They are flat, dome-shaped, pedunculated, and cauliflower-shaped [43]. Clinical presentation includes perianal mass or pain, fistula, abscess, discharge, bleeding, or pruritus [45]. It was noted that recurrence is common [43].

In CT, they appear as soft-tissue density with vascularization [46]. In MRI, they are isointense on T1WIs, slightly hyperintense on T2WIs, with restricted diffusion on DWI, and heterogeneous enhancement after contrast injection (Fig. 15) [46]. Extremely large warts are called Buschke–Lowenstein tumors (giant condyloma acuminata) which are very rare lesions occurring in 0.1% of the population [44, 46]. They usually affect immunocompromised patients and are associated with high malignancy, recurrence, and mortality rates [46]. This disease is considered an intermediate step between squamous carcinoma and condyloma acuminatum, or a benign lesion with a malignant behavior [46]. Moreover, adjuvant chemotherapy is used in addition to the surgery for Buschke–Lowenstein tumors [46].

Fig. 10 46-year-old male presents with right buttock pain. **a** Axial post-contrast CT image of the pelvis showing a large lobulated enhancing mass (white arrow) within the right ischiorectal fossa extending into the right sciatic notch (black arrow). **b–d** Pelvic MRI, Axial T1WI (**b**), T2WI (**c**) and post-contrast T1WI (**d**) show the lobulated mass (white arrow) with low signal in T1WI and high heterogeneous signal in T2WI that presents with intense contrast enhancement (white arrow) in the post-contrast image. Note the displacement of the fat within the left ischiorectal fossa (black arrowhead in (**b**). **e**, **f** Pelvic MRI, Coronal T1WI (**e**) and Sagittal T2WI (**f**) demonstrate the large tumor (white arrows) in the right ischiorectal fossa. Surgical resection confirmed a solitary fibrous tumor (hemangiopericytoma)

Primary malignant neoplasms

Malignant granular cell tumor

Granular cell tumor (GCT) is a rare benign soft-tissue tumor that most probably arises from Schwann cells. Approximately, 0.5–2% of GCTs are malignant [47]. Malignant GCT are aggressive neoplasm with a high rate of metastasis and relapse with a mortality rate of 40–60% [47, 48]. Malignant GCTs can be distinguished from benign GCTs via clinical assessment, in addition to histological examination [47, 49].

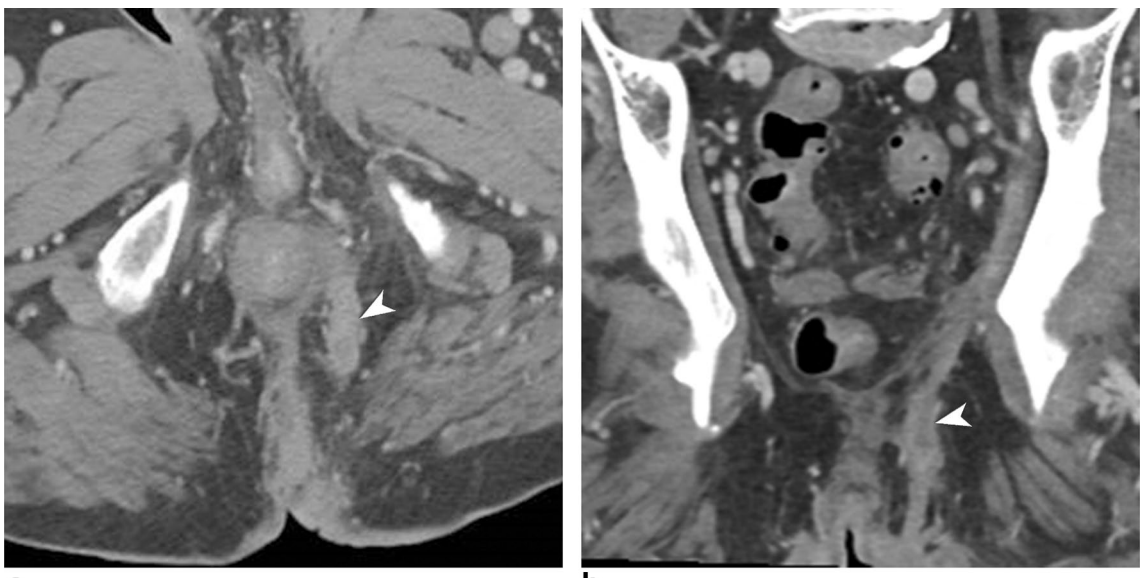

Fig. 9 56-year-old male presents with lower abdominal pain, for which he underwent CT abdomen and pelvis for assessment. Axial (**a**) and reconstructed coronal (**b**) contrast-enhanced CT images of the pelvis showing a large mass-like area (white arrowhead) in the perianal region along the levator ani muscle extending to the subcutaneous tissues representing a hidradenoma papilliferum

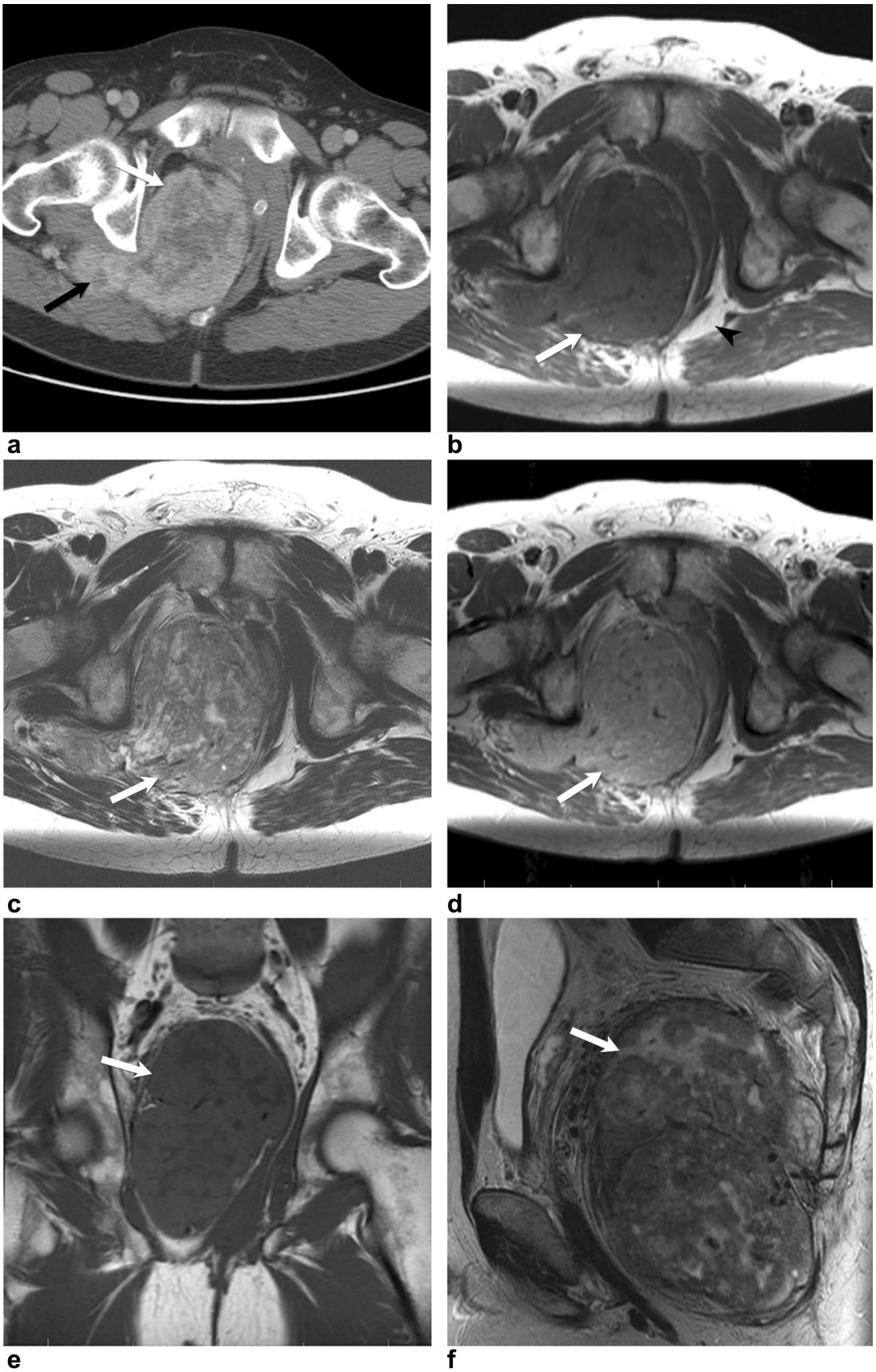
a
b
c
d
e
f

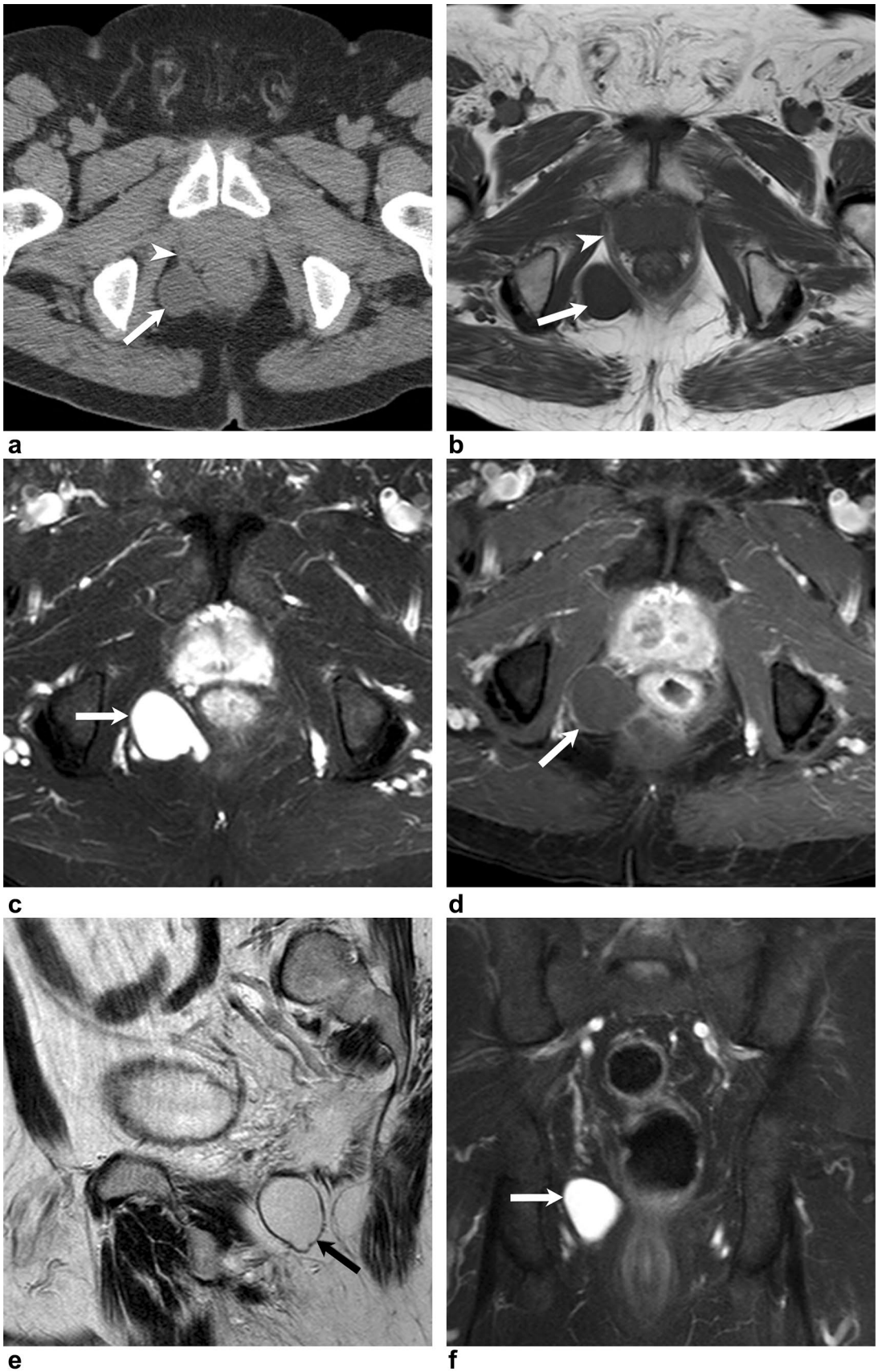
a
b
c
d
e
f

◂**Fig. 11** 68-year-old male with a mass in the tailbone. **a** Axial CT image of the pelvis showing a hypodense lesion (white arrow) in the right ischiorectal fossa lateral to the right levator ani muscle (white arrowhead). **b**, **c** Pelvic MRI, Axial T1WI (**b**) and fat saturated T2WI (**c**) show T1-hypointense and T2-hyperintense, well-circumscribed cystic lesion (white arrows) in the right ischiorectal fossa. **d** Pelvic MRI, Axial post-contrast T1WI demonstrates no enhancement (white arrow) in the mass. **e**, **f** Pelvic MRI, Coronal (**e**) and sagittal (**f**) T2WIs show the lesion (white arrow) within the right ischiorectal fossa representing a tailgut cyst

They commonly present in middle-aged female patients as asymptomatic slowly growing mass [47]. MR features of malignant GCTs include inhomogeneous low to intermediate signal on T1- and T2WIs; in addition to heterogeneous enhancement in T1WIs after gadolinium injection (Fig. 16) [50]. They are treated with wide local excision and regional lymph node dissection. Annual follow-up was suggested to detect any local recurrence which usually precedes metastatic disease [48].

Liposarcoma

Liposarcomas are the second most common soft-tissue sarcoma, after malignant fibrous histiocytoma [20]. Well-differentiated liposarcoma (WDLPS) and dedifferentiated liposarcoma (DDLPS) are the most common histological variants of liposarcoma [51]. WDLPS presents usually as a slowly growing painless mass that doesn't metastasize, while DDLPS is an aggressive high-grade sarcoma that commonly presents with metastases [20].

Although radiological appearance of liposarcoma (Fig. 17) can be similar to lipomas, radiological features suggestive of malignancy include larger lesion size, broader and nodular fibrous septa, mixed fat and non-fatty mass-like lesions, and decrease percentage of fat composition [12, 20]. WDLPS can present with calcification in 10–32% of cases on CT [52].

Enhancing or centrally necrotic nodule is a characteristic feature of DDLPS on CT compared to WDLPS [51]. These lesions are treated with trans-sacral complete surgical resection. In addition, post-operative adjuvant chemotherapy can improve local control and decrease relapse rates. Furthermore, radiotherapy can be added on an individual case basis for high-grade liposarcoma [20].

Leiomyosarcoma

Leiomyosarcoma is a malignant tumor of smooth muscle that may arise from muscularis mucosa, muscularis propria, or the wall of blood vessels [53]. Leiomyosarcomas are exceedingly rare in the perianal area [54]. Mehta and colleagues [54] were first to report a case of leiomyosarcoma in the ischiorectal fossa in 2015 [54]. Leiomyosarcoma is a non-encapsulated well-defined tumor that is formed of sheets of spindle cells with marked nuclear pleomorphism [53, 54].

Leiomyosarcoma presents as a submucosal multilobulated firm mass that can be palpated on digital rectal examination. Although clinical presentation is often indistinguishable from anal SCC, anal leiomyosarcoma is usually symptomatic when small in size because of its close relation to the neural tissue of the anal canal [53]. Leiomyosarcomas are generally heterogeneous on CT. Radiological features in MRI (Fig. 18) include a low signal on T1WI, a heterogeneous high signal on T2WI, and post-contrast enhancement. Surgical resection through combined trans-abdominal and trans-gluteal approaches is the treatment of choice for ischiorectal leiomyosarcoma [54].

Rhabdomyosarcoma

Rhabdomyosarcomas are malignant soft-tissue tumors that are derived from rhabdomyoblasts which are the primitive precursor of skeletal muscle [55]. They account for 5% of childhood malignancies and they rarely present in adults [55]. Abdominopelvic rhabdomyosarcomas commonly involve the external genitalia and paratesticular tissue; perineum and ischiorectal fossa; or the retroperitoneum [26, 55].

Rhabdomyosarcomas in the ischiorectal fossa present as a perineal, genital, or groin swelling [55, 56]. CT depicts the tumor isoattenuating relative to the skeletal muscle with hyperattenuating foci of necrosis and hemorrhage [26]. On MRI, the tumor is isointense to skeletal muscle on T1WIs, and hyperintense to skeletal muscle on T2WIs, with moderate to marked heterogeneous contrast enhancement (Fig. 19). Calcification is a rare feature of rhabdomyosarcoma [55]. Standard management would be surgical excision, followed by radiotherapy and chemotherapy

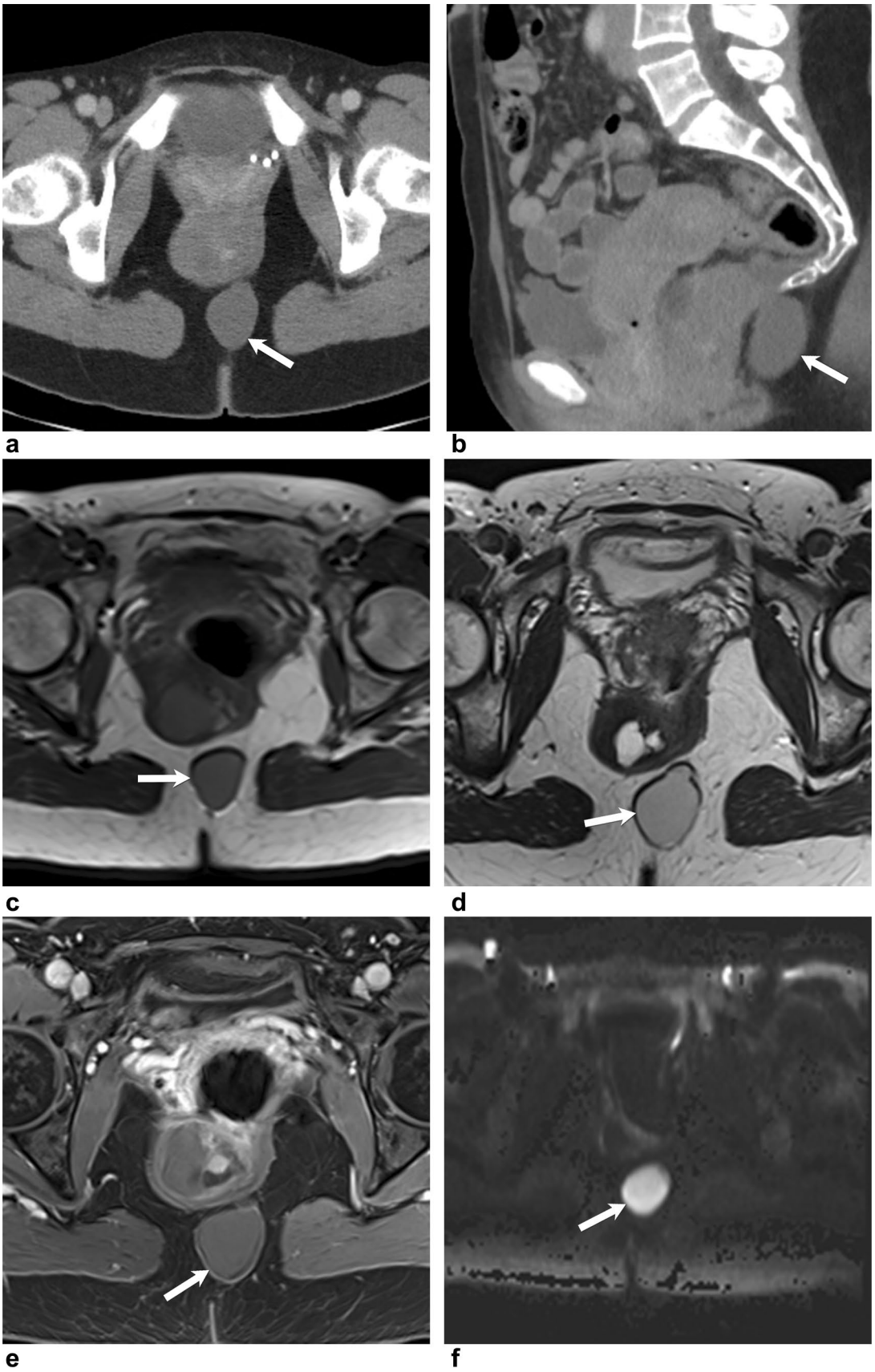
a
b
c
d
e
f

◂**Fig. 12** 51-year-old female with a mass in the coccyx. **a**, **b** Axial (**a**) and sagittal (**b**) CT images of the pelvis showing a hypodense lesion (white arrows). **c**, **d** Pelvic MRI, Axial T1WI (**c**) and T2WI (**d**) show a well-demarcated oval lesion (white arrows) posterior to the anus with an intermediate signal in T1WI and high signal relative to the muscle in T2WIs. **e** Pelvic MRI, Post-contrast fat saturated T1WI (**e**) shows no central enhancement in the aforementioned mass (white arrow) with a peripheral thin rim enhancement after contrast injection. **f** Pelvic MRI, Axial diffusion-weighted image shows restricted diffusion. The mass was surgically removed and confirmed to be an epidermal cyst

[55]. They have a 5-year survival rate of less than 50% [55].

Undifferentiated pleomorphic sarcoma

Twenty percent of soft-tissue sarcoma display no line of histological differentiation and are classified as an undifferentiated sarcoma [26]. Undifferentiated pleomorphic sarcoma (previously known as malignant fibrous histiocytoma) is the most common subtype [26]. It presents usually as painless expanding soft-tissue mass in the lower extremities or retroperitoneum with significant male predominance [57, 58]. Its occurrence in the ischiorectal fossa is extremely uncommon [57]. Grossly they either appear unencapsulated and ill-defined or as a well-defined mass with a pseudocapsule [57].

Clinical presentation of undifferentiated pleomorphic sarcoma is usually non-specific. CT findings include; well-circumscribed mass of soft tissue attenuation with areas of low attenuation in the center representing necrosis or hemorrhage; punctate or coarse calcifications; in addition to variable contrast enhancement [26]. This tumor depicts an intermediate signal in T1WI and T2WI which appears heterogeneous in the presence of hemorrhage, calcifications or necrosis, in addition to prominent enhancement of solid components in post-contrast sequence (Fig. 20). Furthermore, undifferentiated pleomorphic sarcoma is associated with high incidence of hematogenous metastases and local recurrence [57].

Malignant PEComa

The World Health Organization defines PEComa as a mesenchymal tumor that is composed of histologically and immunohistochemically distinctive perivascular epithelioid cell (PEC) [59]. PEComas are a family of mesenchymal tumors including angiomyolipoma, lymphangiomyomatosis, clear cell 'sugar' tumor of the lung, in addition to a group of rare lesions arising at a various visceral and soft

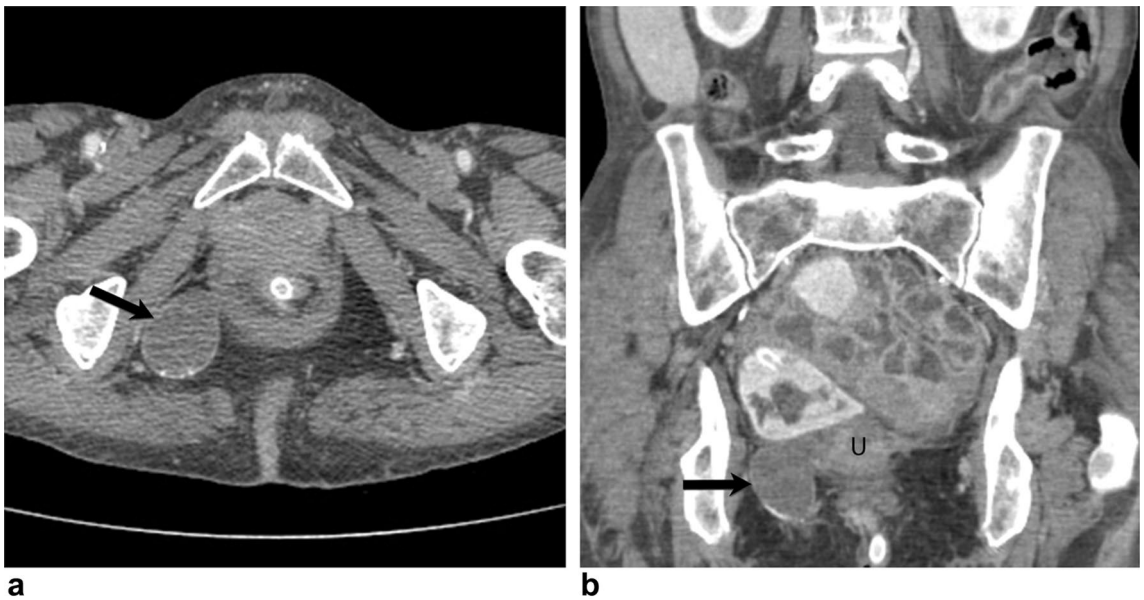

Fig. 13 64-year-old female with chronic abdominal pain underwent follow-up CT scan of the pelvis for suspicious pancreatic changes. Axial (**a**) and coronal (**b**) post-contrast CT images of the pelvis showing a round mass (black arrows) in the right ischiorectal fossa, which has peripheral calcifications. The round mass is contiguous with the uterus (U) representing a pedunculated fibroid

tissue sites [60]. A subset of this family has a malignant behavior [60]. Flope et al. [61] reported that malignant PEComas are associated with tumor size larger than 5 cm, mitotic index more than 1/50 high power field (HPF), high nuclear grade, and necrosis or vascular invasion [61]. Malignant PEComas commonly present in the retroperitoneum, female genital tract, mesentery, or lower extremities [62]. Approximately 72% of malignant PEComas metastasize to distant organs as lung, liver, and peritoneum.

Fig. 15 65-year-old male presents with chronic perineal pain and growing perineal mass. **a** Axial contrast-enhanced CT image of the pelvis showing massive scrotal and perineal condyloma (white arrow) with extension of the condyloma in the bilateral ischiorectal fossae (black arrowheads). **b–d** Pelvic MRI, Axial T1WI (**b**) and T2WI (**c**) and post-contrast T1WI (**d**) show the enormous scrotal and perineal condyloma (white arrows) that appears hypointense on T1 WI and hyperintense on T2WI with enhancement (white arrow) on the post-contrast image. The mass extends into both ischiorectal fossae (white arrowheads). **e**, **f** Pelvic MRI, Coronal (**e**) and sagittal (**f**) T2WIs show the condyloma (white arrows) and its extension into the ischiorectal fossae and represents condyloma acuminata

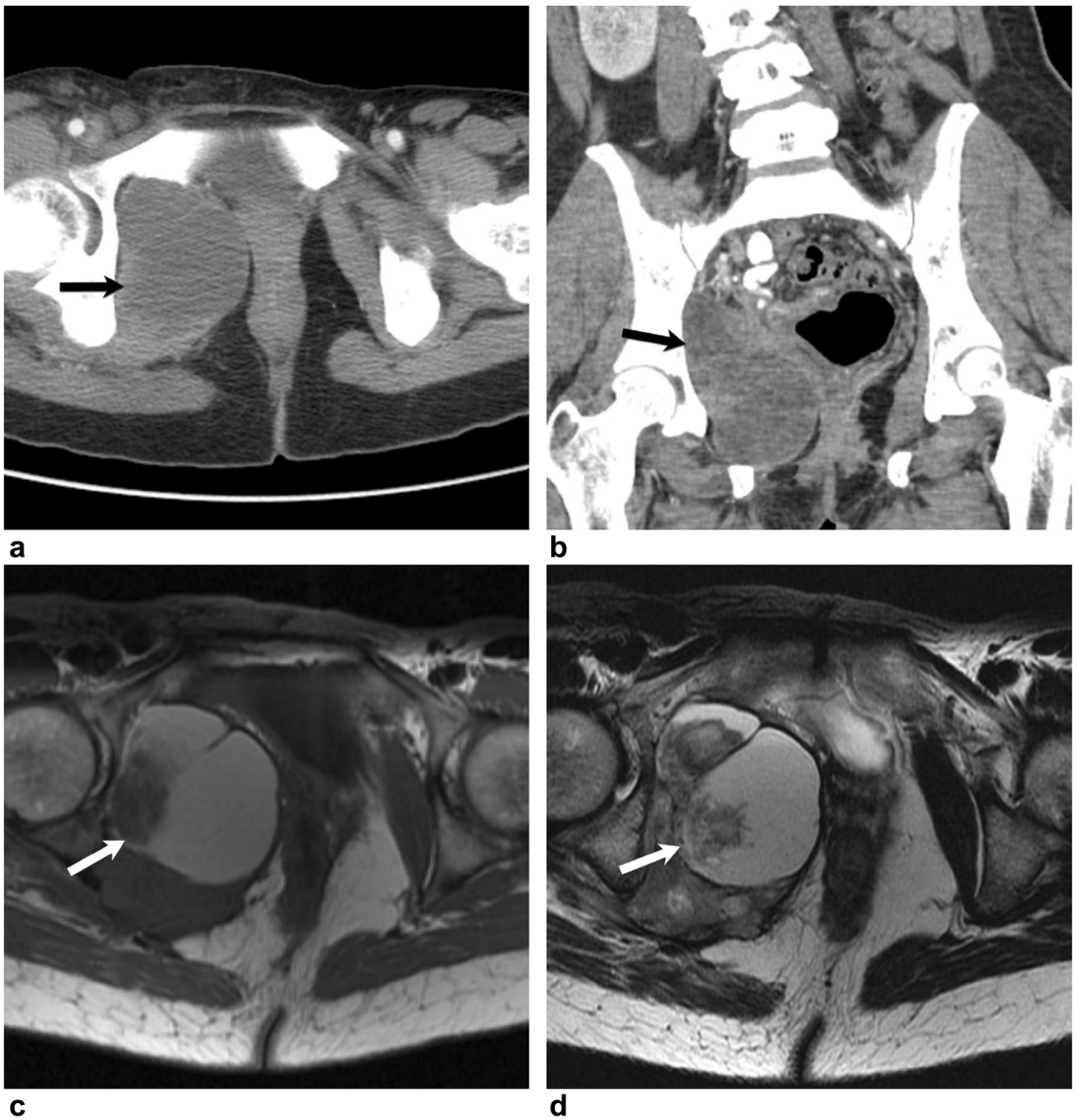

Fig. 14 36-year-old female presented with pelvic pain. **a**, **b** Axial (**a**) and reconstructed coronal (**b**) contrast-enhanced CT images of the pelvis showing a mass in the right ischiorectal fossa (black arrows) which a thin septation. **c**, **d** Pelvic MRI, Axial T1WI (**c**) and T2WI (**d**) show that this lesion (white arrow) has a high signal intensity on the TIWI and T2WI related to blood products representing an endometrioma. Note internal nodularity on the T2WI within the mass (white arrow) which represents adenocarcinoma arising from endometriosis

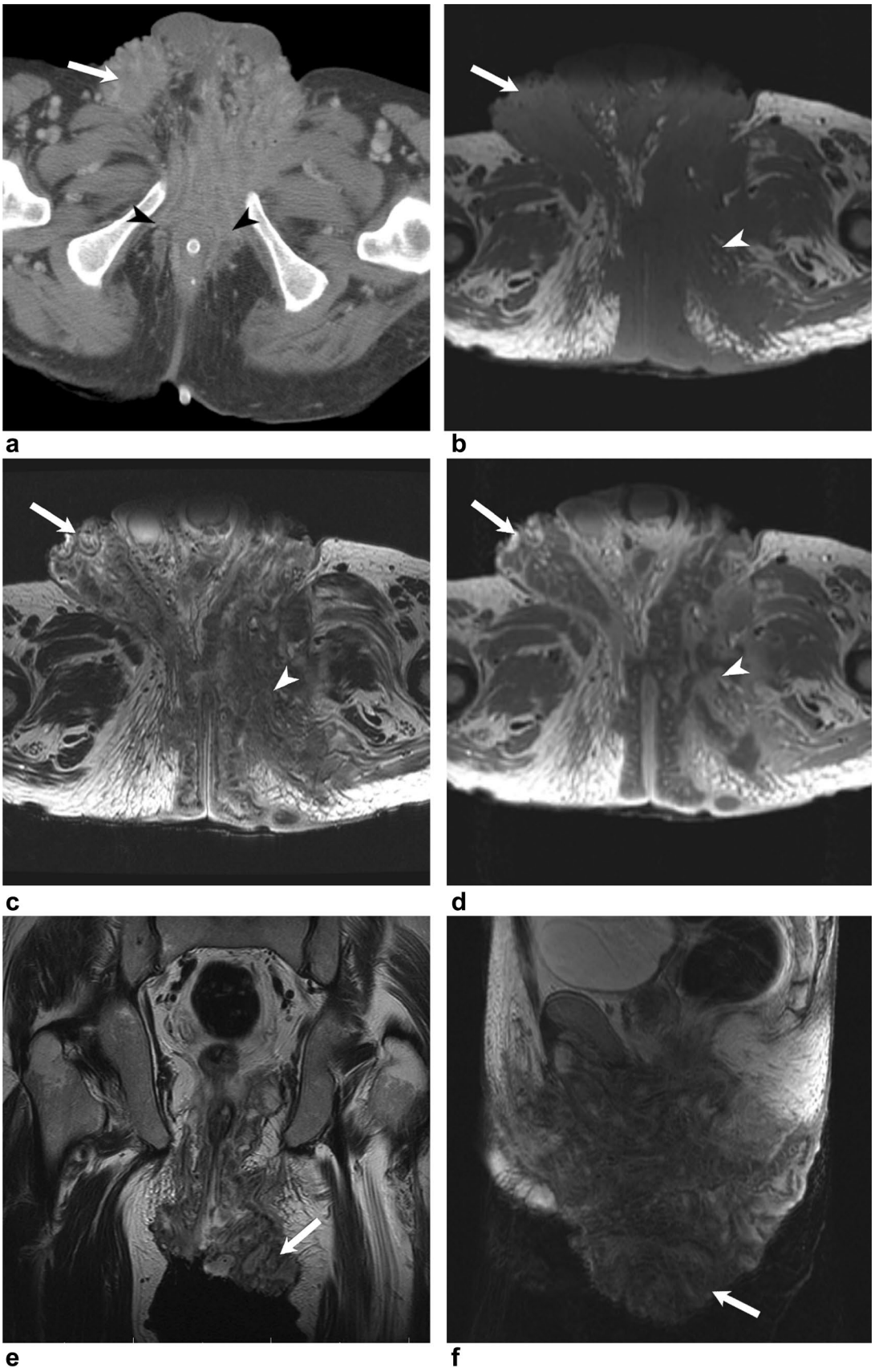
a
b
c
d
e
f

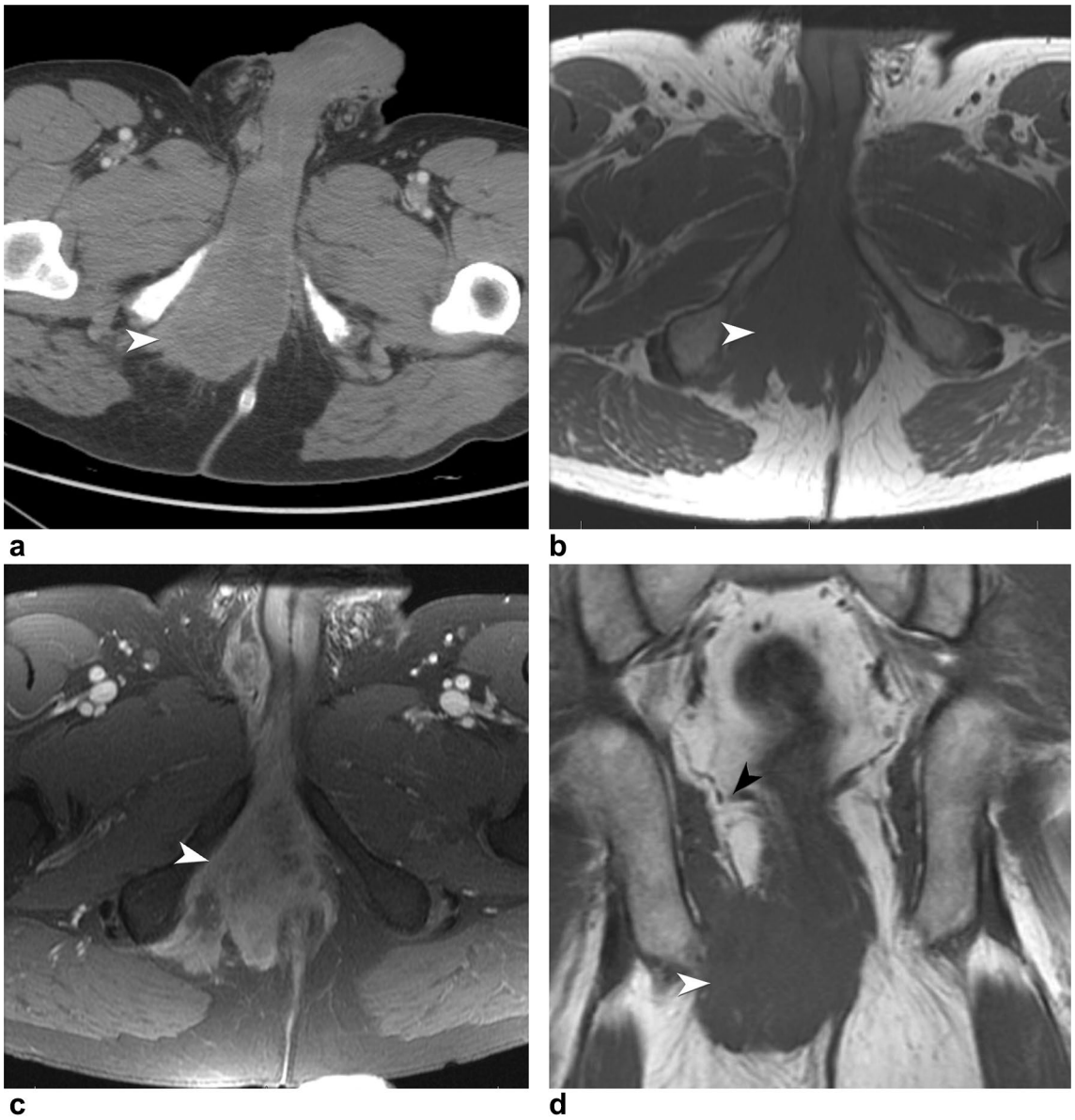

Fig. 16 51-year-old male with right buttock discomfort. **a** Axial post-contrast CT image of the pelvis showing a large hypodense mass (white arrowhead) in the right ischiorectal fossa. **b**, **c** Pelvic MRI, Axial T1WI (**b**) and post-contrast T1WI (**c**) show a mass (white arrowheads) with low signal in T1WI and intense enhancement (white arrowhead) after contrast injection. **d** Pelvic MRI, coronal T2WI shows extension of the mass (white arrowhead) through the right ischiorectal fossa below the levator ani muscle (black arrowhead). This mass was resected with the diagnosis of malignant granular cell tumor

Malignant PEComa is a very aggressive disease and associated with high mortality [62].

Ultrasound reveals heterogeneous echotexture with cystic and necrotic areas in large tumors [62]. On CT, they usually appear as a well-circumscribed soft-tissue mass with hypo- to isodense signal compared to skeletal muscles, with variable post-contrast enhancement (Fig. 21) [62]. While MRI characteristics include hypo- to isointense signal on T1WI; heterogeneous hyperintense signal on T2WI; and variable contrast enhancement [62].

Secondary involvement

Although, hematogenous metastases within the ischiorectal rectal fossa are rare, direct invasion by neoplasms

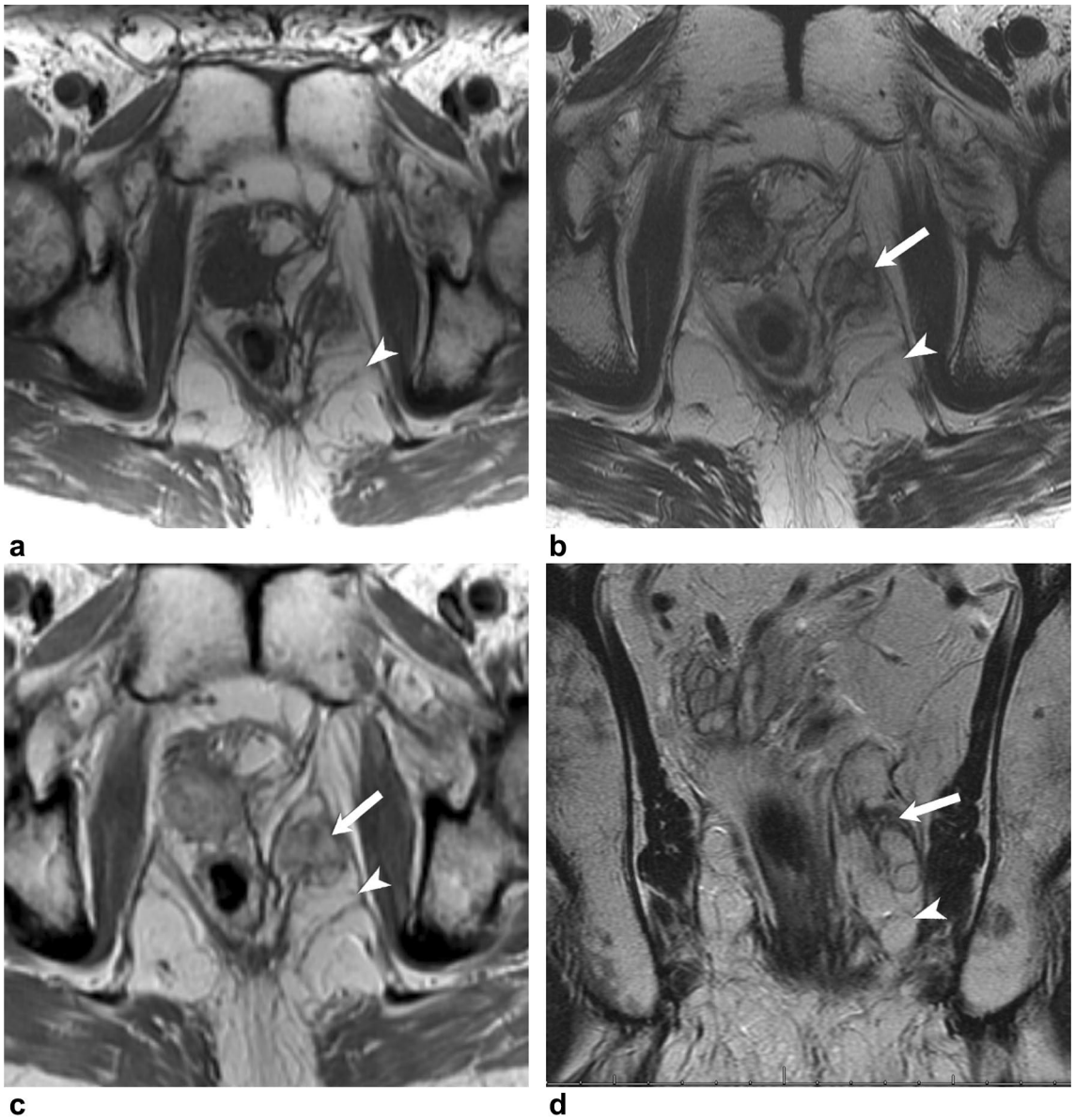

Fig. 17 61-year-old male presents with growing mass in the left perirectal region, for which he underwent pelvic MRI for assessment. **a** Axial T1WI (**a**) showing a fatty mass (white arrowhead) in the left ischiorectal fossa. **b**, **c** Axial T2WI (**b**), and post-contrast axial T1WI (**c**) show the fatty mass (white arrowheads) in the fossa. Low signal intensity soft tissue (white arrows) is noted, which shows contrast enhancement in post-contrast image (**c**). **d** Coronal T2WI (**d**) shows the heterogeneous mass (white arrowhead) containing fat in the left ischiorectal fossa, abutting the rectal wall and extends superiorly above the levator ani muscle. The mass was resected with the diagnosis of liposarcoma

originating from adjacent pelvic organs and structures is commonly encountered. For example, primary tumors from anus, rectum, prostate, or pelvic bone tumors may invade the ischiorectal fossa.

Anorectal cancers

Anal cancers are uncommon with incidence of 1.5–2:100,000 persons per year [63, 64]. It is closely associated with human immune deficiency virus (HIV),

human papillomavirus-16 (HPV-16), immune suppression, and chronic anorectal fistula [2, 63]. 75–95% of anal tumors are squamous cell carcinoma (SCC) [2, 65]. The symptoms include bleeding, perianal mass, pain, itching, ulcer, discharge, or fistula [2, 63]. Anal and lower rectal neoplasms can extend into the ischiorectal fossa (Figs. 22, 23).

MRI is an excellent diagnostic modality for the evaluation of anal cancer with a reported sensitivity of 90–100% [63]. MRI features of the tumor include high signal intensity

Fig. 19 21-year-old male presents with a left buttock pain. **a**, **b** Axial (**a**) and reconstructed coronal (**b**) contrast-enhanced CT images of the pelvis showing large 7.5 × 4.7 cm mass (white arrowhead) in the left ischiorectal fossa with heterogeneous contrast enhancement. **c**, **d** Pelvic MRI, Axial T1WI (**c**) and T2WI (**d**) show a heterogeneous multiloculated mass (white arrowhead) in the left ischiorectal fossa with areas of high signal in T1- and T2WI. **e** Pelvic MRI, Axial post-contrast T1WI depicts contrast enhancement (white arrowhead) in the mass. **f** Pelvic MRI, Coronal T2WI shows the large heterogeneous mass (white arrowhead) that was resected with the diagnosis of rhabdomyosarcoma. Fluid–fluid levels are noted in the mass likely related to internal hemorrhage ▶

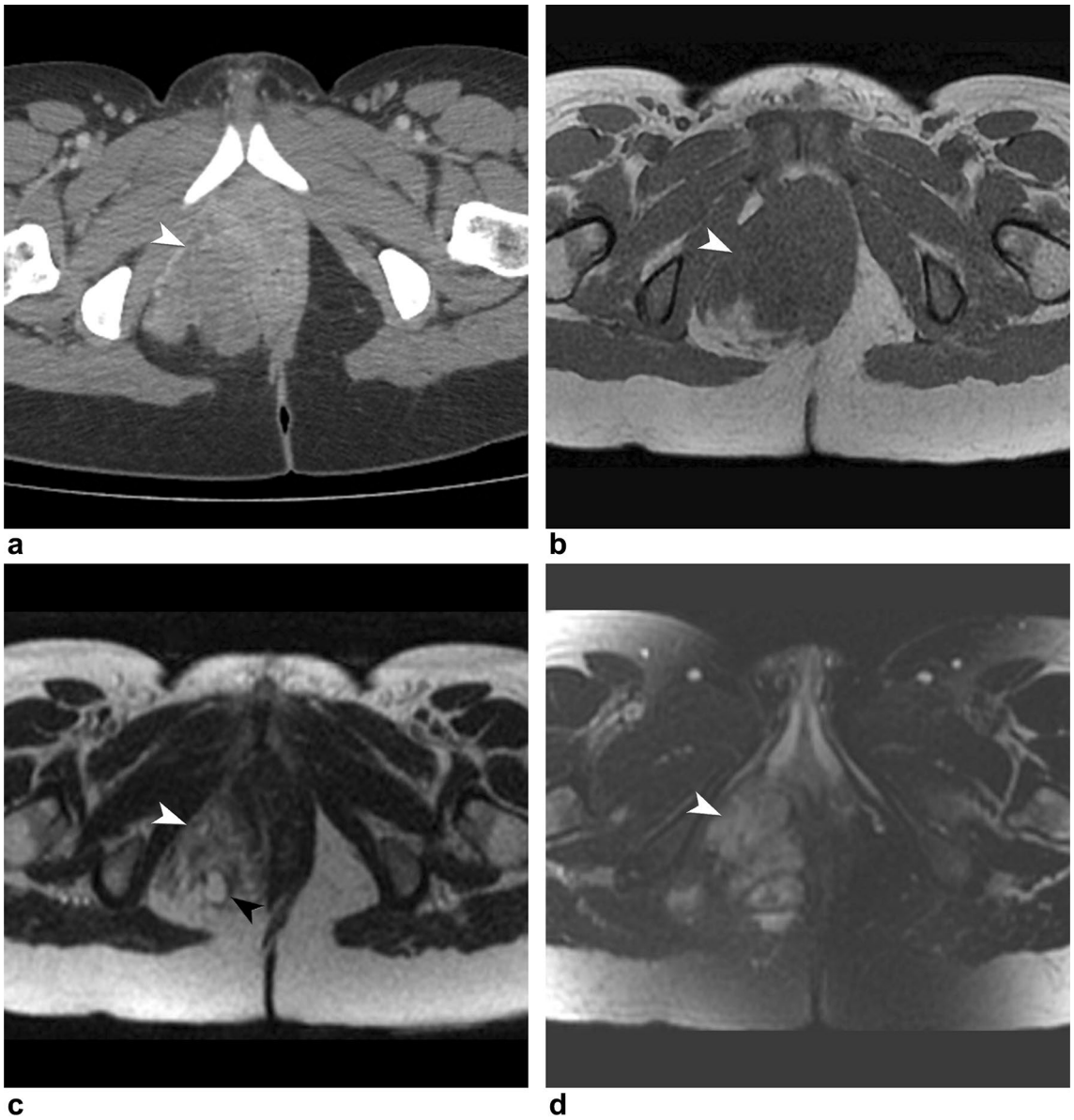

Fig. 18 34-year-old female presents with nausea and bloating for which an abdominal ultrasound was performed and revealed a pelvic mass. She underwent CT and MRI for further assessment. **a** Axial contrast-enhanced CT image of the pelvis showing a 6.6 cm mass in the right ischiorectal fossa (white arrowhead) with heterogeneous contrast enhancement. **b**–**d** Pelvic MRI, Axial T1WI (**b**), T2WI (**c**) and post-contrast T1WI (**d**) show that the mass (white arrowheads) presents with a low signal in T1WI, a heterogeneous high signal in T2WI and with enhancement on the post-contrast image. Areas of increased T2 signal are noted on the T2 weighted images representing myxoid tissue (black arrowhead). The mass was resected with the diagnosis of myxoid leiomyosarcoma

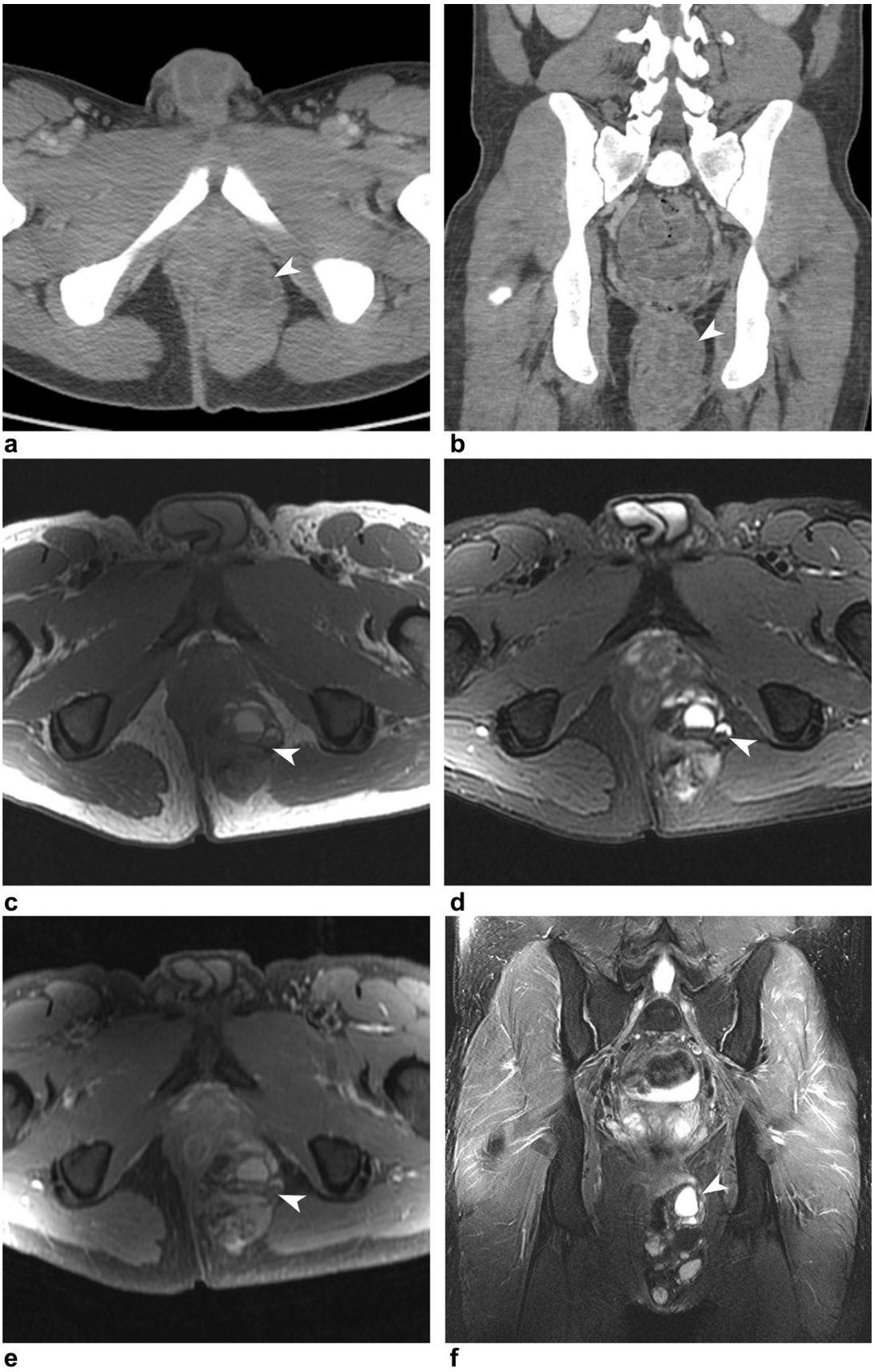
a
b
c
d
e
f

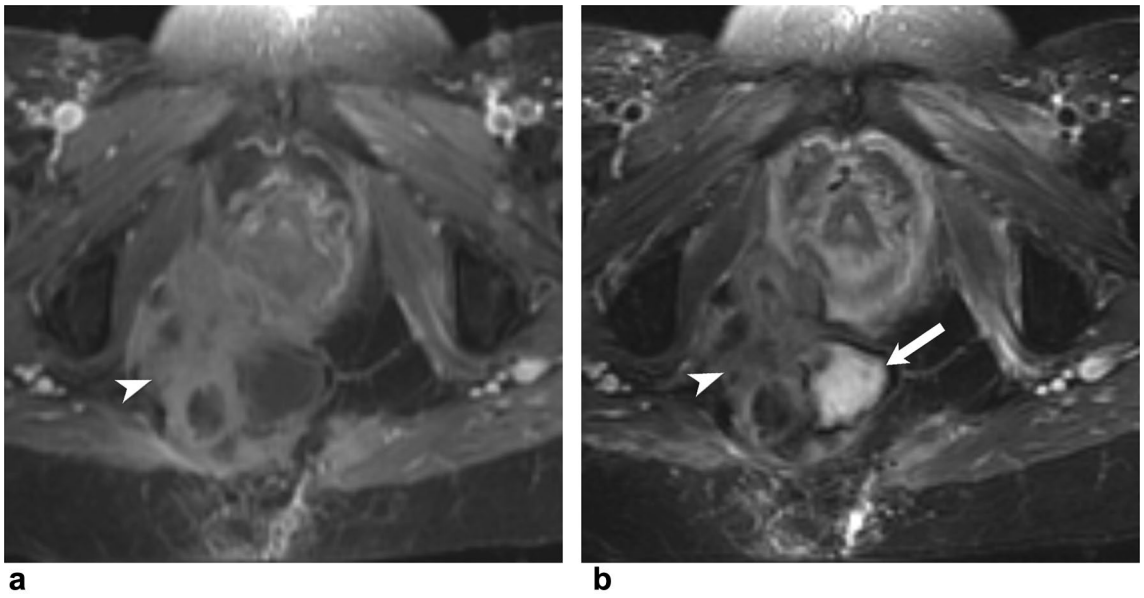

Fig. 20 52-year-old female presents with right buttock pain. Axial post-contrast T1WI (**a**) and fat sat T2WI (**b**) showing an enhancing pelvic mass (white arrowheads) that fills the entire right ischiorectal fossa. The tumor involves the lower sacrum and the surrounding muscles. Areas of increased signal noted on the T2WI (white arrow) represent cystic changes within the lesion suggesting necrosis. The tumor was proven to be undifferentiated pleomorphic sarcoma (malignant fibrous histiocytoma) after surgical excision

Fig. 21 69-year-old female presents with buttock discomfort while sitting. Axial precontrast (**a**) and contrast-enhanced (**b**) CT images of the pelvis show the large hypodense mass (white arrowheads) within the left ischiorectal fossa with mild enhancement after IV injection of contrast (**b**). The mass was resected with the diagnosis of high-grade malignant PEComa

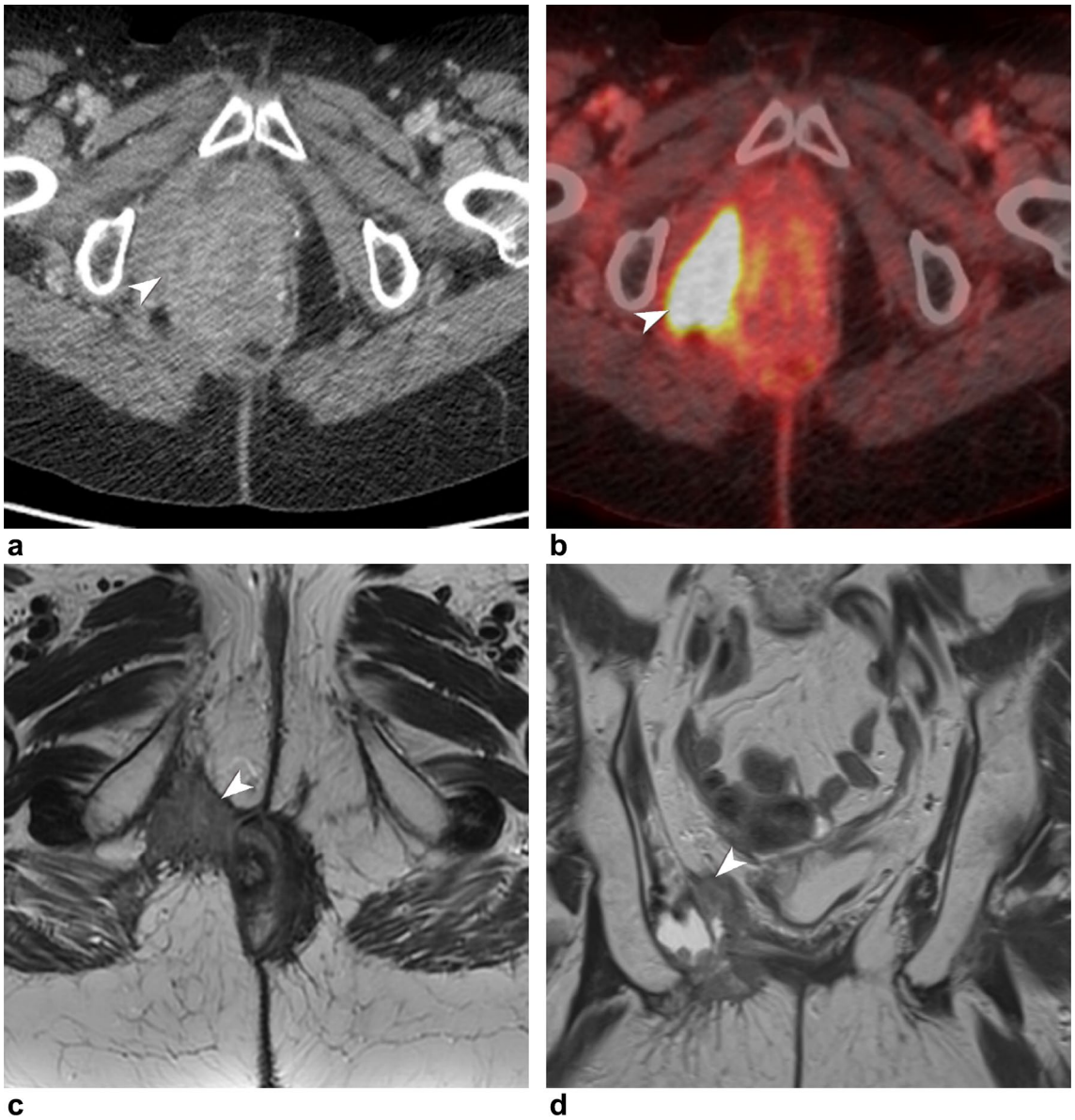

Fig. 22 76-year-old male with anal squamous cell carcinoma, status post abdominoperineal resection, presents for surveillance. **a** Axial post-contrast CT image of the pelvis showing a soft tissue area with enhancement (white arrowhead) within the right ischiorectal fossa. **b** Axial PET/CT image of the pelvis shows the mass with high FDG uptake (white arrowhead). **c** Pelvic MRI, Axial T2WI demonstrates hyperintense mass in the right ischiorectal fossa. **d** Pelvic MRI, Axial post-contrast T1WI shows the mass heterogeneously enhancing (white arrowhead) in the soft tissue area suspicious for recurrent tumor. The recurrent tumor extends into the ischiorectal fossa

compared to the nearby muscles in T2WIs; low to intermediate signal intensity on T1WI; and marked enhancement with gadolinium injection [63]. CT demonstrates non-enhancing iso- or hypodense anal mass with peripheral calcification that can extend into the ischiorectal fossa [2]. Asymmetric sphincteric or levator ani thickness, and linear stranding in the ischiorectal fossa are indicative of local tumor spread [66]. They are usually FDG-avid [63, 67].

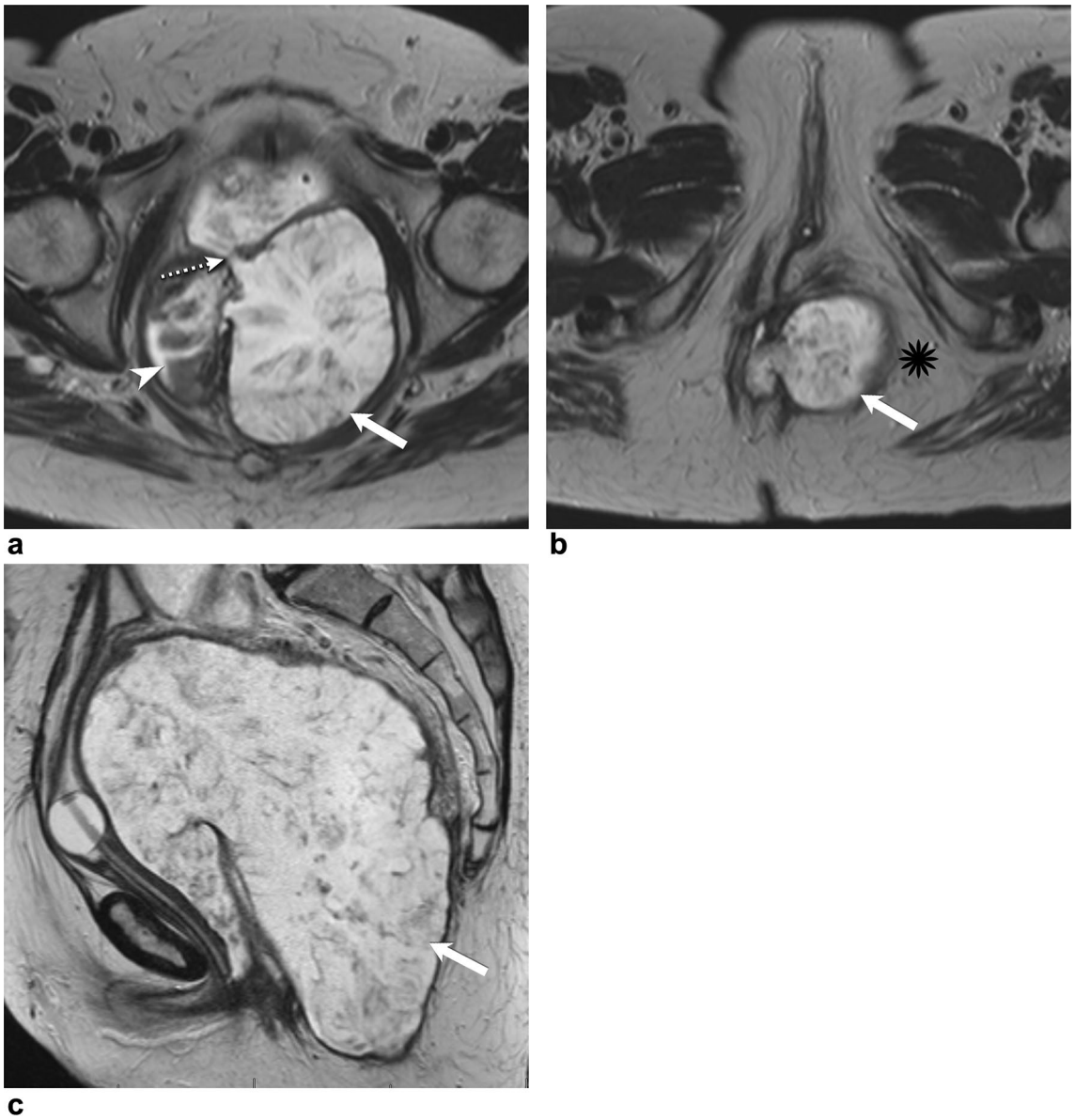

Fig. 23 55-year-old female with locally advanced rectal adenocarcinoma on chemotherapy. She underwent pelvic MRI for assessment. Axial (**a**, **b**) and Sagittal (**c**) T2WI demonstrating a large polypoid rectal mass (white arrowhead) with a huge perirectal mucinous component (white arrow) that measures 15×7.5×3.8 cm. This tumor passes through the internal and external anal sphincter and extends into the left ischiorectal fossa (black asterisk) and left perineum resulting in a rectoperineal fistula. The mass invades the vagina and there is a fistulas communication with the vagina (dotted white arrow)

Metastatic disease

Hematogenous metastases of extrapelvic malignancies to the ischiorectal fossa are rare, but some tumors such as melanoma (Fig. 24), lymphoma (Fig. 25), gastro-intestinal stromal tumor and chordoma among others may give mestatases to the ischiorectal fossa [2].

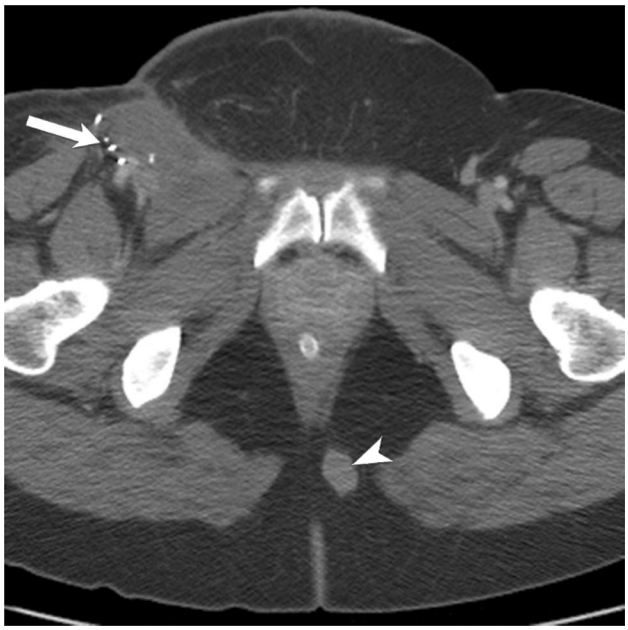

Fig. 24 48-year-old female with melanoma of the right thigh status post-surgical resection and right inguinal lymph node dissection. Axial contrast-enhanced CT image of the pelvis showing metastatic lesion (white arrowhead) in the left ischiorectal fossa, in addition to the site of nodal dissection (white arrow)

Chordoma

Chordomas are very uncommon bone tumors that arise usually from the sacrum, skull base, and spine with 50% arising in the sacrococcygeal region [10, 68]. They are thought to have an embryological origin from the primitive notochord [68]. Although they are low-grade, they can rarely undergo aggressive sarcomatous or dedifferentiated high-grade differentiation [68]. Clinical presentation includes symptoms of mass effect or local invasion [10].

On CT, chordoma appears as a heterogeneous, lobulated, lytic soft-tissue mass with intramural calcifications in the ischiorectal fossa [10, 12]. MR features include hyperintense presacral mass on T2WIs due to mucin content with hypointense foci due to hemosiderin; predominantly hypointense signal on T1WIs with some hyperintense regions due to hemorrhage; in addition to variable enhancement pattern (Fig. 26) [10]. Radiological images can also show destruction of the coccyx, displacement of the rectum or extension into surrounding structures [2]. They are treated with APR and radiotherapy [68]. Sacrococcygeal chordomas have a high rate of local relapse, nearly 46–70% [10].

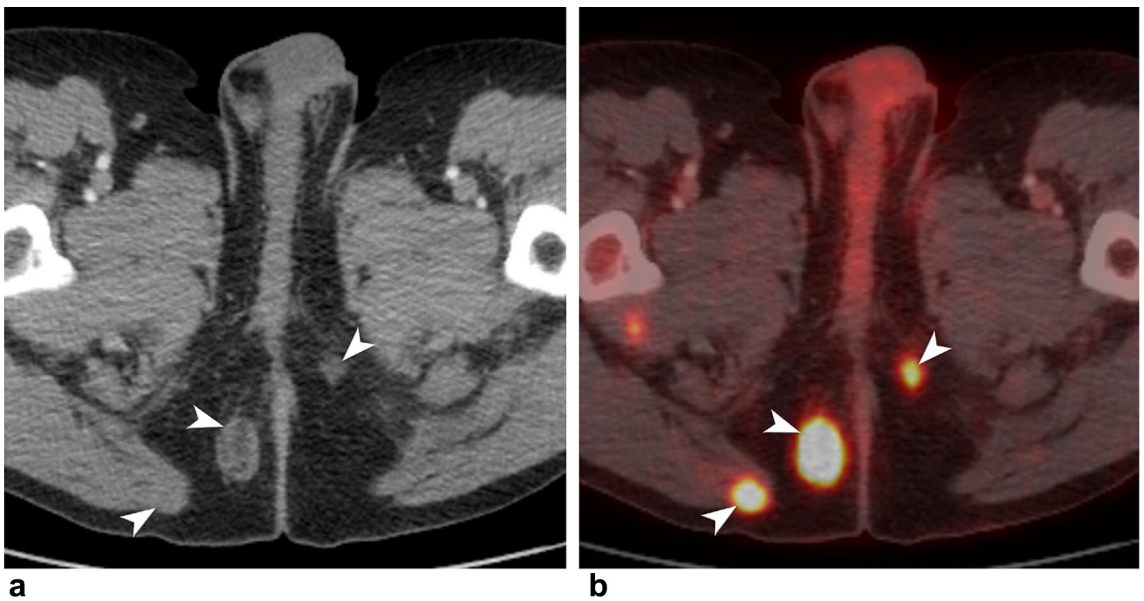

Fig. 25 75-year-old male with lymphoma. Axial contrast-enhanced CT (**a**) and PET/CT (**b**) images of the pelvis showing multiple lymphomatous metastatic masses (white arrowheads) within the bilateral ischiorectal fossae with intense FDG uptake in the PET/CT image (**b**)

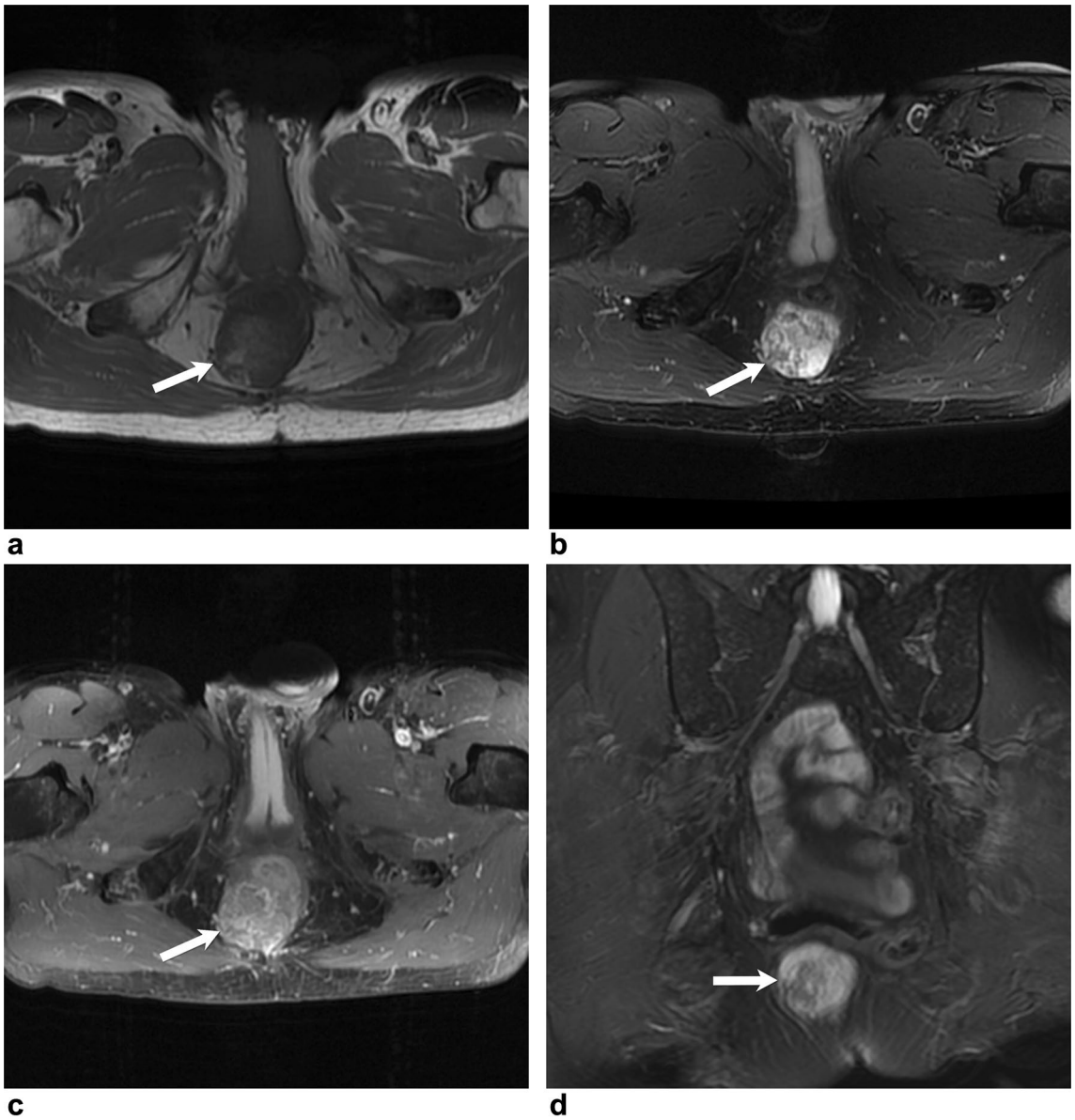

Fig. 26 51-year-old male with a previous resected sacral chordoma, now presenting with pelvic discomfort. He underwent pelvic MRI for assessment. **a**, **b** Axial T1WI (**a**) and T2WI (**b**) show a 2.9 cm mass (white arrows) within the ischiorectal fossa abutting the anus, with low signal in T1WI and high signal in T2WI. **c** Axial post-contrast T1WI depicts contrast enhancement within the mass (white arrow). **d** Coronal T2WI demonstrates the recurrent chordoma (white arrow)

Conclusion

A plethora of pathological conditions can involve the ischiorectal fossa. Most tumors in the ischiorectal fossa arise from its contents such as fat, muscles, vessels, or the adjacent bones. The ischiorectal fossa can also be involved by direct invasion from neoplasms originating in adjacent organs and structures. Additionally, some congenital and infectious/inflammatory lesions and more rarely, metastases, can also occur in the ischiorectal fossa. Imaging plays a key role in the characterization and assessment of ischiorectal fossa lesions. Although, some lesions affecting the ischiorectal fossa may not be distinguished from one another based unically in imaging features and biopsy is needed for a definitive diagnosis, knowledge of the ischiorectal fossa anatomy, and of the spectrum of imaging findings of common and uncommon benign and malignant neoplasm of the ischiorectal fossa is crucial for the radiologists during interpretation of images and differential diagnosis contributing to better patient management.

Acknowledgement We thank Kelly Kage, medical illustrator at MD Anderson Cancer Center for the illustration provided in this article.

Compliance with ethical standards

Conflict of interest The authors declare that they have no disclosure or conflict of interests.

Ethical approval No IRB approval was required.

References

1. Moore KL, Dalley AF, Agur AMR (2014) Clinically oriented anatomy. 7th edn. Williams & Wilkins, Baltimore
2. Llauger J, Palmer J, Perez C, Monill JM, Ribe J, Moreno A (1998) The normal and pathologic ischiorectal fossa at CT and MR imaging. Radiographics 18 (1):61–82. https://doi.org/10.1148/radiographics.18.1.9460109
3. Hoeffel C, Crema MD, Azizi L, Lewin M, Monnier-Cholley L, Arrive L, Tubiana JM (2007) Magnetic resonance imaging of the ischiorectal fossa: spectrum of disease. J Comput Assist Tomogr 31 (2):251–257. https://doi.org/10.1097/01.rct.0000236419.90019.40
4. Hammer RP, Shrewsbury MM (1977) A reconsideration of the ischiorectal fossa. Diseases of the Colon & Rectum 20 (8):681–689. https://doi.org/10.1007/bf02586690
5. Abu JI, Bamford WM, Malin G, Brown L, Davies Q, Ireland D (2005) Aggressive angiomyxoma of the perineum. International Journal of Gynecological Cancer 15 (6):1097–1100. https://doi.org/10.1111/j.1525-1438.2005.00182.x
6. Satheshkumar T, Saklani AP, Banerjee D, Jones DRB (2003) Angiomyofibrosarcoma: A rare ischiorectal fossa swelling. Hospital Medicine 64 (4):244-245
7. Jeyadevan NN, Sohaib SAA, Thomas JM, Jeyarajah A, Shepherd JH, Fisher C (2003) Imaging Features of Aggressive Angiomyxoma. Clinical Radiology 58 (2):157–162. https://doi.org/10.1053/crad.2002.1127
8. Kransdorf MJ, Jelinek JS, Moser RP, Jr., Utz JA, Brower AC, Hudson TM, Berrey BH (1989) Soft-tissue masses: diagnosis using MR imaging. AJR American journal of roentgenology 153 (3):541–547. https://doi.org/10.2214/ajr.153.3.541
9. Surabhi VR, Garg N, Frumovitz M, Bhosale P, Prasad SR, Meis JM (2014) Aggressive angiomyxomas: a comprehensive imaging review with clinical and histopathologic correlation. AJR American journal of roentgenology 202 (6):1171–1178. https://doi.org/10.2214/AJR.13.11668
10. Hosseinzadeh K, Heller MT, Houshmand G (2012) Imaging of the female perineum in adults. Radiographics 32 (4):E129–E168. https://doi.org/10.1148/rg.324115134
11. Arneja JS, Gosain AK (2008) Vascular malformations. Plastic and Reconstructive Surgery 121 (4):195E–206E. https://doi.org/10.1097/01.prs.0000304607.29622.3c
12. Arbelo-Cruz N, Lisanti C, Walker K, Schwope R, Bui-Mansfield LT, Reiter M (2016) Anatomy and Pathology of the Ischiorectal Fossa. Contemporary Diagnostic Radiology 39 (17):1–7. https://doi.org/10.1097/01.CDR.0000490026.20869.7b
13. Ros PR, Eshaghi N (1991) Plexiform neurofibroma of the pelvis: CT and MRI findings. Magnetic Resonance Imaging 9 (3):463–465. https://doi.org/10.1016/0730-725X(91)90436-P
14. Jett K, Friedman JM (2010) Clinical and genetic aspects of neurofibromatosis 1. Genetics in Medicine 12 (1):1–11. https://doi.org/10.1097/GIM.0b013e3181bf15e3
15. Halefoglu AM (2012) Neurofibromatosis type 1 presenting with plexiform neurofibromas in two patients: MRI features. Case Reports in Medicine 2012:1–3. https://doi.org/10.1155/2012/498518
16. Mazzola CR, Power N, Bilsky MH, Robert R, Guillonneau B (2014) Pudendal schwannoma: A case report and literature review. Can Urol Assoc J 8 (3-4):E199–203. https://doi.org/10.5489/cuaj.1734
17. Majbar A, Hrora A, Jahid A, Ahallat M, Raiss M (2016) Perineal schwannoma. BMC research notes 9 (1):304. https://doi.org/10.1186/s13104-016-2108-1
18. Pantè S, Terranova M-L, Leonello G, Fedele F, Ascenti G, Famulari C (2009) Perineal schwannoma. Canadian Journal of Surgery 52 (1):E8–E9
19. Chen S, Gaynor B, Levi AD (2016) Transischiorectal fossa approach for resection of pudendal nerve schwannoma: case report. J Neurosurg Spine 25 (5):636–639. https://doi.org/10.3171/2016.4.SPINE151449
20. Munk PL, Lee MJ, Janzen DL, Connell DG, Logan PM, Poon PY, Bainbridge TC (1997) Lipoma and liposarcoma: Evaluation using CT and MR imaging. American Journal of Roentgenology 169 (2):589–594
21. SScurry J, Van Der Putte SCJ, Pyman J, Chetty N, Szabo R (2009) Mammary-like gland adenoma of the vulva: Review of 46 cases. Pathology 41 (4):372–378. https://doi.org/10.1080/00313020902884493
22. Filho EFA, de Carvalho AL, de Oliveira Costa PF, de Carvalho AC (2016) Resection of ischiorectal fossa tumors – surgical technique. Journal of Coloproctology 36 (3):179–183. https://doi.org/10.1016/j.jcol.2016.04.006
23. Chen X, Wu JT (2017) Imaging findings of big hidradenoma papilliferum in ischiorectal fossa: a case report. INTERNATIONAL JOURNAL OF CLINICAL AND EXPERIMENTAL MEDICINE 10 (8):12693–12697
24. Handa Y, Yamanaka N, Inagaki H, Tomita Y (2003) Large Ulcerated Perianal Hidradenoma Papilliferum in a Young Female. Dermatologic Surgery 29 (7):790–792. https://doi.org/10.1046/j.1524-4725.2003.29201.x
25. Yap T, Hamzah L, Oshowo A, Taylor I (2003) Myxoid solitary fibrous tumour of the ischiorectal fossa. European Journal of Surgical Oncology 29 (1):98–100. https://doi.org/10.1053/ejso.2002.1400
26. Levy AD, Manning MA, Miettinen MM (2017) Soft-Tissue Sarcomas of the Abdomen and Pelvis: Radiologic-Pathologic Features, Part 2-Uncommon Sarcomas. Radiographics 37 (3):797–812. https://doi.org/10.1148/rg.2017160201
27. Chun HJ, Byun JY, Jung SE, Kim KH, Shinn KS (1998) Benign solitary fibrous tumour of the pre-sacral space: MRI findings. British Journal of Radiology 71 (846):677–679. https://doi.org/10.1259/bjr.71.846.9849394
28. Vossough A, Torigian DA, Zhang PJ, Siegelman ES, Banner MP (2005) Extrathoracic solitary fibrous tumor of the pelvic peritoneum with central malignant degeneration on CT and MRI. Journal of Magnetic Resonance Imaging 22 (5):684–686. https://doi.org/10.1002/jmri.20433
29. Zhang W-d, Chen J-y, Cao Y, Liu Q-y, Luo R-g (2011) Computed tomography and magnetic resonance imaging findings of solitary fibrous tumors in the pelvis: Correlation with histopathological findings. European Journal of Radiology 78 (1):65–70. https://doi.org/10.1016/j.ejrad.2009.09.001
30. Shin SS, Jeong YY, Kang HK (2008) Myxoid solitary fibrous tumor of the retroperitoneum: MRI findings with the pathologic correlation. Korean J Radiol 9 (3):279–282. https://doi.org/10.3348/kjr.2008.9.3.279
31. Menassa-Moussa L, Kanso H, Checrallah A, Abboud J, Ghossain M (2005) CT and MR findings of a retrorectal cystic hamartoma

confused with an adnexal mass on ultrasound. European Radiology 15 (2):263–266. https://doi.org/10.1007/s00330-004-2330-4
32. Yang DM, Park CH, Jin W, Chang SK, Kim JE, Choi SJ, Jung DH (2005) Tailgut Cyst: MRI Evaluation. AJR American journal of roentgenology 184 (5):1519-1523
33. Sritharan K, Ghani Y, Thompson H (2014) An unusual encounter of an epidermoid cyst. BMJ case reports 2014 (may13 1):bcr2014204186. https://doi.org/10.1136/bcr-2014-204186
34. Kesici U, Sakman G, Mataraci E (2013) Retrorectal/Presacral epidermoid cyst: report of a case. The Eurasian journal of medicine 45 (3):207–210. https://doi.org/10.5152/eajm.2013.40
35. Fujimoto H, Murakami K, Kashimada A, Terauchi M, Ozawa K, Nosaka K, Arimizu N (1993) Large epidermal cyst involving the ischiorectal fossa: MR demonstration. Clinical Imaging 17 (2):146-148. https://doi.org/10.1016/0899-7071(93)90056-S
36. Kransdorf MJ, Jelinek JS, Moser RP, Jr., Utz JA, Brower AC, Hudson TM, Berrey BH (1989) Soft-tissue masses: diagnosis using MR imaging. AJR Am J Roentgenol 153 (3):541–547. https://doi.org/10.2214/ajr.153.3.541
37. Kim HK, Kim SM, Lee SH, Racadio JM, Shin MJ (2011) Subcutaneous epidermal inclusion cysts: Ultrasound (US) and MR imaging findings. Skeletal Radiology 40 (11):1415–1419. https://doi.org/10.1007/s00256-010-1072-4
38. Deshmukh SP, Gonsalves CF, Guglielmo FF, Mitchell DG (2012) Role of MR imaging of uterine leiomyomas before and after embolization. Radiographics 32 (6):E251–E281
39. Casillas J, Joseph RC, Guerra Jr JJ (1990) CT appearance of uterine leiomyomas. Radiographics 10 (6):999–1007
40. Kim HG, Song YJ, Na YJ, Choi OH (2013) A case of torsion of a subserosal leiomyoma. J Menopausal Med 19 (3):147–150. https://doi.org/10.6118/jmm.2013.19.3.147
41. Odobasic A, Pasic A, Iljazovic-Latifagic E, Arnautalic L, Odobasic A, Idrizovic E, Dervisefendic M, Dedić L (2010) Perineal endometriosis: a case report and review of the literature. Techniques in Coloproctology 14 (S1):25–27. https://doi.org/10.1007/s10151-010-0642-8
42. Chene G, Darcha C, Dechelotte P, Mage G, Canis M (2007) Malignant degeneration of perineal endometriosis in episiotomy scar, case report and review of the literature. International Journal of Gynecological Cancer 17 (3):709–714. https://doi.org/10.1111/j.1525-1438.2007.00822.x
43. Wiley DJ, Douglas J, Beutner K, Cox T, Fife K, Moscicki A-B, Fukumoto L (2002) External Genital Warts: Diagnosis, Treatment, and Prevention. Clinical Infectious Diseases 35 (2):S210–S224. https://doi.org/10.1086/342109
44. Billingham RP, Isler JT, Kimmins MH, Nelson JM, Schweitzer J, Murphy MM (2004) The diagnosis and management of common anorectal disorders. Current Problems in Surgery 41 (7):586–645. https://doi.org/10.1016/j.cpsurg.2004.04.002
45. Trombetta LJ, Place RJ (2001) Giant condyloma acuminatum of the anorectum: Trends in epidemiology and management: Report of a case and review of the literature. Diseases of the Colon & Rectum 44 (12):1878–1886. https://doi.org/10.1007/BF02234473
46. Nelson Montaña C, Labra A, Schiappacasse G (2014) Giant condyloma acuminatum (Buschke-Lowenstein tumor). Series of seven cases and review of the literature. Revista Chilena de Radiología 20 (2):57-63
47. Singh VA, Gunasagaran J, Pailoor J (2015) Granular cell tumour: malignant or benign? SINGAPORE MEDICAL JOURNAL 56 (9):513–517. https://doi.org/10.11622/smedj.2015136
48. Nasser H, Ahmed Y, Szpunar SM, Kowalski PJ (2011) Malignant granular cell tumor: a look into the diagnostic criteria. Pathol Res Pract 207 (3):164–168. https://doi.org/10.1016/j.prp.2010.12.007
49. Fanburg-Smith JC, Meis-Kindblom JM, Fante R, Kindblom LG (1999) Malignant granular cell tumor of soft tissue - Diagnostic criteria and clinicopathologic correlation, (vol 22, pg 779, 1998). AMERICAN JOURNAL OF SURGICAL PATHOLOGY 23 (1):136
50. Osanai T, Ishikawa A, Ogino T, Yamakawa M (2004) Contrast-enhanced magnetic resonance imaging of malignant granular cell tumor with pathological correlation: a case report. Journal of Orthopaedic Science 9 (5):529–532. https://doi.org/10.1007/s00776-004-0814-3
51. Bhosale P, Wang J, Varma D, Jensen C, Patnana M, Wei W, Chauhan A, Feig B, Patel S, Somaiah N, Sagebiel T (2016) Can abdominal computed tomography imaging help accurately identify a dedifferentiated component in a well-differentiated liposarcoma? Journal of Computer Assisted Tomography 40 (6):872–879. https://doi.org/10.1097/RCT.0000000000000462
52. Gupta P, Potti TA, Wuertzer SD, Lenchik L, Pacholke DA (2016) Spectrum of fat-containing soft-tissue masses at MR imaging: The common, the uncommon, the characteristic, and the sometimes confusing. Radiographics 36 (3):753–766. https://doi.org/10.1148/rg.2016150133
53. Wang TK, Chung MT (1998) Anorectal leiomyosarcomas. Journal of gastroenterology 33 (3):402–407
54. Mehta N, Konarski A, Rooney P, Chandrasekar C (2015) Leiomyosarcoma of the ischiorectal fossa: report of a novel sphincter and sciatic nerve sparing simultaneous trans-abdominal and trans-gluteal resection and review of the literature. J Surg Case Rep 2015 (3):rjv016–rjv016. https://doi.org/10.1093/jscr/rjv016
55. Reisner D, Amadi C, Beckman I, Patel S, Surampudi R (2014) Pelvic alveolar rhabdomyosarcoma in a young adult. Radiol Case Rep 9 (4):798. https://doi.org/10.2484/rcr.v9i4.798
56. Agrons GA, Wagner BJ, Lonergan GJ, Dickey GE, Kaufman MS (1997) From the archives of the AFIP. Genitourinary rhabdomyosarcoma in children: radiologic-pathologic correlation. Radiographics 17 (4):919–937. https://doi.org/10.1148/radiographics.17.4.9225391
57. Stever MR, Hernandez E, Sakas EL (1988) Malignant fibrous histiocytoma of the pelvis. Gynecologic Oncology 30 (2):285–290. https://doi.org/10.1016/0090-8258(88)90034-0
58. Mohan RP, Verma S, Siddhu VK, Agarwal N (2013) Malignant fibrous histiocytoma. BMJ Case Rep 2013. https://doi.org/10.1136/bcr-2013-008875
59. Fletcher CD, Bridge JA, Hogendoorn PC, Mertens F (2013) WHO classification of tumours of soft tissue and bone. IARC Press, Lyon
60. Hornick JL, Fletcher CDM (2006) PEComa: what do we know so far? Histopathology 48 (1):75–82. https://doi.org/10.1111/j.1365-2559.2005.02316.x
61. Folpe AL, Mentzel T, Lehr HA, Fisher C, Balzer BL, Weiss SW (2005) Perivascular epithelioid cell neoplasms of soft tissue and gynecologic origin: a clinicopathologic study of 26 cases and review of the literature. Am J Surg Pathol 29 (12):1558–1575
62. Tirumani SH, Shinagare AB, Hargreaves J, Jagannathan JP, Hornick JL, Wagner AJ, Ramaiya NH (2014) Imaging Features of Primary and Metastatic Malignant Perivascular Epithelioid Cell Tumors. AMERICAN JOURNAL OF ROENTGENOLOGY 202 (2):252–258. https://doi.org/10.2214/AJR.13.10909
63. Durot C, Dohan A, Boudiaf M, Servois V, Soyer P, Hoeffel C (2017) Cancer of the Anal Canal: Diagnosis, Staging and Follow-Up with MRI. Korean J Radiol 18 (6):946–956. https://doi.org/10.3348/kjr.2017.18.6.946
64. Granata V, Fusco R, Reginelli A, Roberto L, Granata F, Rega D, Rotondo A, Grassi R, Izzo F, Petrillo A (2016) Radiological assessment of anal cancer: an overview and update. INFECTIOUS AGENTS AND CANCER 11 (1):1–9. https://doi.org/10.1186/s13027-016-0100-y
65. Roy AC, Wattchow D, Astill D, Singh S, Pendlebury S, Gormly K, Segelov E (2017) Uncommon Anal Neoplasms. SURGICAL ONCOLOGY CLINICS OF NORTH AMERICA 26 (1):143. https://doi.org/10.1016/j.soc.2016.07.009

66. Scherrer A, Reboul F, Martin D, Dupuy JC, Menu Y (1990) CT of malignant anal canal tumors. Radiographics 10 (3):433–453. https://doi.org/10.1148/radiographics.10.3.2188307
67. Mahmud A, Poon R, Jonker D (2017) PET imaging in anal canal cancer: a systematic review and meta-analysis. BRITISH JOURNAL OF RADIOLOGY 90 (1080). https://doi.org/10.1259/bjr.20170370
68. Casali PG, Stacchiotti S, Sangalli C, Olmi P, Gronchi A (2007) Chordoma. Current Opinion in Oncology 19 (4):367–370. https://doi.org/10.1097/CCO.0b013e3281214448